

4D Printing: Towards Biomimetic Additive Manufacturing

Elizabeth Yinling Tsai

B.S. as recommended by the Department of Materials Science & Engineering
& in Engineering as recommended by the Department of Mechanical Engineering
Massachusetts Institute of Technology (2011)

Submitted to the Program in Media Arts and Sciences, School of Architecture and
Planning, in partial fulfillment of the requirements for the degree of

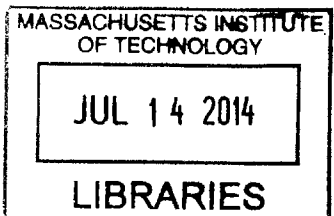
Master of Science in Media Arts & Sciences

at the

Massachusetts Institute of Technology

September 2013

ARCHIVES



© Massachusetts Institute of Technology 2012. All rights reserved.

Signature redacted

Author: _____

Elizabeth Yinling Tsai
Program in Media Arts and Sciences

August 9, 2013

Signature redacted

Certified by: _____

Prof. Neri Oxman
Assistant Professor of Media Art and Sciences
Program in Media Arts and Sciences

Thesis Advisor

Signature redacted

Accepted by: _____

Prof. Patricia Maes
Associate Academic Head
Program in Media Arts and Sciences

4D Printing: Towards Biomimetic Additive Manufacturing

Elizabeth Yinling Tsai

Submitted to the Program in Media Arts and Sciences, School of Architecture and Planning, on August 9, 2013 in partial fulfillment of the requirements for the degree of Master of Science in Media Arts & Science at the Massachusetts Institute of Technology

Abstract

Inherent across all scales in Nature's material systems are multiple design dimensions, the existences of which are products of both evolution and environment. In human manufacturing where design must be preconceived and deliberate, static artifacts with no variation of function across directions, distances or time fail to capture many of these dimensions. Inspired by Nature's ability to generate complex structures and responses to external constraints through adaptation, "4D printing" addresses additive fabrication of artifacts with *one or more additional design dimension*, such as material variation over distance or direction and response or adaptation over time. This work presents and evaluates a series of enabling explorations into the material, time and information dimensions of additive manufacturing: a variable elasticity rapid prototyping platform and an approach towards Digital Anisotropy, a variable impedance prosthetic socket (VTS) as a case study of interfaces between nature and manufacture, CNSilk as an example of on-demand material generation in freeform tensile fabrication, and Material DNA as an exploration into embedded spatio-temporal content variation.

This work was supported in part by NSF EAGER grant award #1152550 "Bio-Beams: Functionally Graded Rapid Design & Fabrication", VA contract # VA118-12-C-0040, and the Media Lab Consortium.

Thesis Advisor: Dr. Neri Oxman

Title: Assistant Professor of Media Arts and Sciences, Program in Media Arts and Sciences

4D Printing: Towards Biomimetic Additive Manufacturing

Elizabeth Yinling Tsai

Submitted to the Program in Media Arts and Sciences, School of Architecture and
Planning, in partial fulfillment of the requirements for the degree of
Master of Science in Media Arts & Science

Signature rédacted

Thesis Reader: _____

Hugh Herr
Associate Professor of Media Arts and Sciences
Program in Media Arts and Sciences

4D Printing: Towards Biomimetic Additive Manufacturing

Elizabeth Yinling Tsai

Submitted to the Program in Media Arts and Sciences, School of Architecture and
Planning, in partial fulfillment of the requirements for the degree of
Master of Science in Media Arts & Science

Signature redacted

Thesis Reader: _____

Edward Boyden
Associate Professor of Media Arts and Sciences
Program in Media Arts and Sciences

Acknowledgements

My past six years at MIT, and in particular the most recent two at the Media Lab, have played a major role in making me who I am as an individual, researcher and engineer. There have been countless individuals who have contributed deeply to this journey of learning and personal growth – certainly more than I have been able to mention here. To all of you, I would like to say thank you with the utmost sincerity. Nothing would have been possible without each of you.

Neri Oxman, my advisor, for giving me a chance and for being an incredibly open and encouraging mentor. Thank you for continuously pushing me to see and think about the world in new ways.

My thesis readers, **Hugh Herr** and **Ed Boyden** for their input and discourse. Thank you for taking the time.

The Mediated Matter group: **Steven Keating**, **Ben Peters**, **Michal Firstenberg**, **Yoav Sterman**, **Carlos Gonzales**, **Markus Keyser** and **Jared Laucks** for being invaluable team mates and colleagues as well as **Zjenja Doubrovski** and **Federico Mazzolini** for the many engaging discussions and insights.

Phil Salesses, my best friend, above all for believing in me and always being there.

The people who make what we do possible: **Sarah Ryan** who has been more amazing than we thought possible, **Cynthia Wilkes** for being so willing to aid and assist, and the indefatigable **Linda Peterson** for putting up with all of us year after year. **Tom Lutz** and **John Difrancesco** in the shop for being so patient and capable.

Stratasys and **Daniel Dikovsky** who made the translation from concept to reality possible across such short timelines.

Arthur Petron and **David Sengeh** from the Biomechatronics Group for the invaluable discussions, input and advice.

My wonderful UROPs, in particular **Ben Lehnert**, who remind me how little I know and motivate me to always continue to learn.

My former UROP mentor, **Nate Reticker-Flynn**. You exemplify a degree of dedication to mentoring and research that I will only ever aspire to. **Prof. Sang-Gook Kim** for revealing to me a first glimpse of the world of research and **Prof. Yoel Fink** for taking the time to care and offer words of wisdom.

And then, most certainly, my parents, **Rose Lee** and **Eric Tsai**, as well as my brother, **Enoch**, for helping me get here in the first place and for their unquestionable love and support.

Table of Contents

1. INTRODUCTION & BACKGROUND.....	10
1.1 MOTIVATION & LIMITATIONS OF CURRENT ADDITIVE MANUFACTURING	10
1.2 4D PRINTING: TOWARDS BIOMIMETIC ADDITIVE MANUFACTURING	10
1.3 STATE OF THE ART IN 3D PRINTING	11
1.4 4D EXAMPLES IN CURRENT MANUFACTURING.....	12
1.5 THESIS ORGANIZATION.....	13
2. APPROACH & METHODOLOGY.....	15
2.1 METHODOLOGY	15
2.2 NATURE'S WAY: BIOLOGICAL PARALLELS FOR ADDITIVE MANUFACTURING	15
2.2.1 <i>Aggregate Systems</i>	16
2.2.2 <i>Tensile Web and Membrane Systems</i>	17
2.2.3 <i>Cellular Compressive Systems</i>	19
2.2.4 <i>Cellular Tensile Systems</i>	19
2.3 DEFINING THE 4 TH DIMENSION	20
2.3.1 <i>In Nature</i>	20
2.3.2 <i>In Layered Manufacturing</i>	20
2.3.2.1 The Material Dimension.....	20
2.3.2.2 The Time Dimension.....	22
2.3.2.3 The Information Dimension	22
2.4 INTERFACING BETWEEN NATURE AND ADDITIVE MANUFACTURING.....	23
3. IMPLEMENTATION	25
3.1 OVERVIEW	25
3.2 THE MATERIAL DIMENSION: DIRECTION & DISTANCE	25
3.2.1 <i>Vision: Adaptation of Composition & Form</i>	25
3.2.2 <i>Digital Anisotropy: A Variable Elasticity Rapid Prototyping Platform</i>	26
3.2.2.1 Motivation	26
3.2.2.2 Design and Control	27
3.2.2.3 Gradient Fabrication.....	31
3.2.2.3 <i>Physical Interfaces: Variable Impedance Test Socket</i>	34
3.2.3.1 Motivation & Background.....	34
3.2.3.2 Process Overview.....	36
3.2.3.3 Data Collection.....	38
3.2.3.4 Modeling.....	42
3.2.3.5 Material Mapping	45
3.2.3.6 Shape Determination.....	46
3.2.3.7 File Generation	47
3.2.3.8 Socket Fabrication	50
3.2.3 <i>Physical Interfaces: Variable Impedance Test Socket</i>	34
3.2.3.1 Motivation & Background.....	34
3.2.3.2 Process Overview.....	36
3.2.3.3 Data Collection.....	38
3.2.3.4 Modeling.....	42
3.2.3.5 Material Mapping	45
3.2.3.6 Shape Determination.....	46
3.2.3.7 File Generation	47
3.2.3.8 Socket Fabrication	50
3.3 THE TIME DIMENSION: GROWTH AND RESPONSE	53
3.3.1 <i>Vision: Fabrication Material Behavior & Response</i>	53
3.3.2 <i>On-demand Material Generation: CNSilk</i>	53
3.3.2.1 Overview & Motivation.....	54
3.3.2.2 Design.....	55
3.3.2.3 Material Generation: Nylon 6,6	56
3.3.2.4 Discussion & Realization.....	59
3.3.3 <i>Environmental Response: Passive Smart Glass</i>	60
3.4 THE INFORMATION DIMENSION: SPATIO-TEMPORAL CONTENT VARIATION.....	62

3.4.1 Vision: Materials As Software.....	62
3.4.2 Embedding Information: Material DNA.....	62
4. EVALUATION & CONTRIBUTIONS.....	65
4.1 THEORY & METHODOLOGY: EXPLORATION OF ADDITIONAL FABRICATION DIMENSIONS....	65
4.1.1 Nature: Growth, Adaptation, Evolution	65
4.1.2 Manufacture: Defining The 4 th Dimension.....	65
4.2 TECHNOLOGY	65
4.2.1 Object Representation: Bitmap Printing	65
4.2.2 Platforms: CNSilk and Variable Elasticity Printer.....	66
4.2.3 Systems: Material DNA	66
4.3 IMPLICATIONS IN DESIGN AND FABRICATION	66
5. CONCLUSIONS.....	68
REFERENCES.....	69

List of Figures

FIGURE 1. ADAPTATION OF COMPOSITION AND FORM IN NATURE'S MATERIAL SYSTEMS.....	16
FIGURE 2. ENVIRONMENTAL SCANNING ELECTRON MICROGRAPHS OF SPIDER SILK FIBERS).	18
FIGURE 3. COMPOSITE IMAGE OF CARPAL SKIN.....	21
FIGURE 4. VARIABLE ELASTICITY PRINTING PLATFORM.....	27
FIGURE 5. VARIABLE ELASTICITY PRINTING PLATFORM: TOP VIEW	28
FIGURE 6. VARIABLE ELASTICITY PRINTING PLATFORM: SOLENOID VALVES AND MATERIAL RESERVOIRS	29
FIGURE 7. VARIABLE ELASTICITY PRINTING PLATFORM: PASSIVE MIXER.....	29
FIGURE 8. VARIABLE ELASTICITY PRINTING PLATFORM: COLOR GRADIENTS.....	32
FIGURE 9. VARIABLE ELASTICITY PRINTING PLATFORM: CAST SILICONE SHEET.	32
FIGURE 10. VARIABLE ELASTICITY PRINTING PLATFORM: UV CURE SILICONE AND POLYURETHANE SAMPLES TESTED ...	33
FIGURE 11. VARIABLE ELASTICITY PRINTING PLATFORM: TWO-DIMENSIONAL GRADIENTS	34
FIGURE 12. VTS: DESIGN AND FABRICATION PROCESS	37
FIGURE 13. VTS: IMAGES FROM MRI SCAN OF A RIGHT RESIDUAL LIMB	39
FIGURE 14. VTS: TISSUE DISPLACEMENT VS TISSUE THICKNESS	40
FIGURE 15. VTS: STIFFNESS VS TISSUE THICKNESS	41
FIGURE 16. VTS: ORIGIN AND AXIS FOR DATA STRUCTURE.	42
FIGURE 17. VTS: RENDERINGS.	46
FIGURE 18. VTS: DETERMINING SOCKET SHAPE	47
FIGURE 19. VTS: BITMAP FILES.....	50
FIGURE 20. VTS: PRINTED SOCKET	51
FIGURE 21. VTS: COMPOSITE SHELL DESIGN	52
FIGURE 22. VTS: COMPOSITE SHELL LAYUP	52
FIGURE 23. CNSILK: KUKA ATTACHMENT.....	56
FIGURE 24. CNSILK: NYLON 6,6 SYNTHESIS.....	57
FIGURE 25. CNSILK: ROBOTIC ARM WEAVING	58
FIGURE 26. CNSILK: NYLON 6,6 MEMBRANES	59
FIGURE 27. PASSIVE SMART GLASS EXAMPLE	61
FIGURE 28. MATERIAL DNA PARTICLES.....	63

1. Introduction & Background

1.1 Motivation & Limitations of Current Additive Manufacturing

State of the art additive-manufacturing platforms typically utilize a wide variety of materials and combinations of materials to 3D print objects with complex geometries. Typically necessitated by the fabrication process itself, such objects are fabricated in a layer-by-layer method (Levy, Schindel, & Kruth, 2003). Although some work has been done towards heterogeneous object modeling in layered manufacturing (Patil, Dutta, Bhatt, Jurrens, Lyons, & Pratt, 2002), variations in bulk material properties or anisotropies of the object are often byproducts of the fabrication itself (Ahn, Montero, Odell, Roundy, & Wright, 2002) (Cooke, Tomlinson, Burguete, Johns, & Vanard, 2011).

Currently, the most accessible approaches to the fabrication of designed anisotropy are achieved through the introduction of spatial non-uniformity in material composition (Oxman, Keating, & Tsai, 2011). Tangible examples include the optimization of cellular material distributions and density in response to loading patterns on the architectural scale as well as geometrical and material gradients of varying elasticity on product scale applications (Oxman, Tsai, & Firstenberg, 2012). Such efforts enable the user to design, control and modulate properties across spatial and temporal scales, designing both material and organization.

1.2 4D Printing: Towards Biomimetic Additive Manufacturing

In moving towards the nexus of biomimetic fabrication and additive manufacturing, several limitations arise in prototyping with current methods and materials. Static objects with no functional variation across directions, distances or time fail to capture many of the intricacies inherent across different scales in Nature's designs. As concrete examples: orthoses and prostheses intended to interface intimately with the human form embody intricate geometries yet are typically composed of a number of homogenous materials. Given that the shape and

volume of human limbs fluctuate during each step and throughout different levels of activity due in part to muscle contractions and other forces there is real need for artifacts that are able to comfortably accommodate this broad range of movements.

This thesis introduces the term “4D printing” addresses the rapid fabrication of artifacts with one or more additional design dimensions. In particular, 4D printing is defined as the fabrication of objects through the deposition of a material using a print head, nozzle, or other printer technology where the objects contain one or more additional design dimension, such as material gradation over distance or direction, response or adaptation over time, or controlled anisotropy throughout volume.

1.3 State of the Art in 3D Printing

Additive and layered manufacturing systems allow for objects of varying complexity to be serially produced in a one-off fashion from 3D model data. Using a single manufacturing system, a large number of unique objects may be fabricated without additional molds or tooling, though support materials may sometimes be used (Weiss, et al., 1997). Examples of layered manufacturing include fused deposition modeling (FDM), selective laser sintering (SLS), stereolithography (SLA), laminated object manufacturing (LOM), and 3D printing. Each method is typically limited in the materials that it may fabricate with depending on the Nature of the process and post-processing steps. An FDM printer, for example, may print with thermoplastic materials as well as a water- soluble material, the latter of which is later removed. With the exception of Stratasys’ simultaneous multi-material jetting technology commercial methods are limited in the range of achievable material properties and are generally unable to combine different materials within a single printed model.

Advances in commercial additive manufacturing technologies often occur in one of two directions: increased resolution or material developments. FDM methods developed by Stratasys, for example, extrude thermoplastic materials while multiple

material photolithography platforms such as the Objet500 Connex Multi-Material Printer are able to duplicate a wide range of material properties such as stiffness, tensile strength, durometer, opacity and color using its Digital Materials (Stratasys). Methods such as electron beam melting and direct metal laser sintering can work with metal materials while other SLS machines can print with wider ranges of commercially available powder materials ranging from plastics to ceramics and glass. Technologies developed more recently in research stages work with biological materials and scaffolds as they seek to expand from the nanoscale to the architectural scale (Buswell, Soar, Gibb, & Thorpe, 2007) (Melchels, Feijen, & Grijpma, 2010).

1.4 4D Examples in Current Manufacturing

With current additive manufacturing methods, there has been some exploration of material property and response modulation as functions of direction, distance, and time. Instances of this may be seen in materials with specifically manufactured anisotropic properties, passive responsive materials, and graded material distributions. Concepts of 4D printing are embodied in examples of functionally graded rapid prototyping (FGRP) and variable property rapid prototyping (VPRP) for example (Miyamoto, Kaysser, Rabin, Kawasaki, & Ford, 1999) (Weiss, et al., 1997) (Oxman, 2010). In both FGRP and VPRP, the assignment of material properties and distribution are modulated as a function of either distance or direction. By enabling the design of functional structural components through the controlled spatial variation of material properties in continuous gradients, they result in structures highly optimized to fit environmental performance requirements (Oxman, 2011) (Oxman, Keating, & Tsai, 2011). Digital Anisotropy then allows for the control of both density and directionality of material substance as well as property across multiple scales and locations.

Beyond material variations, other examples focus on event-specific interactions with the environment post-fabrication. Work on printed origami

explores structure periodicity and the transition between dimensionality, where multiple structures can be created from a single printed lattice design through different folding pathways (Ahn, Montero, Odell, Roundy, & Wright, 2002). Certain multivascular self-healing materials respond to crack-induced rupture of embedded capsules – and hence the material itself – with automatic repair (Toohey, Sottos, Lewis, Moore, & White, 2007).

In a more deliberate sense, structures and devices may be fabricated with specific dynamic functions, as with electrically small 3D antennas (Adams, et al., 2011). Using conventionally fabricated shape changing materials such as shape memory alloys and polymers assembled with 3D printed parts, smart actuators, structures, and mechanisms may be produced (Walters & Rossiter, 2008) with applications in soft robotics (Rossiter, Walters, & Stoimenov, 2009) and art and design (Walters & McGoran, 2011). Most recently, the rapid prototyping of artifacts designed to self-assemble or undergo specific transformations post-fabrication has emerged (Tibbits, 2013). With such smart structures, external stimuli function not only as a trigger event but also provide the energy necessary for actuation.

1.5 Thesis Organization

This thesis is composed of five chapters. *Chapter 1: Introduction & Background* discusses the limitations of current additive manufacturing, introduces the concept of 4D printing, and examines the state of the art in 3D printing. *Chapter 2: Approach & Methodology* describes the systematic method used in the exploration of 4D printing and presents a series of biological parallels for additive manufacturing present in Nature. It seeks to define the 4th dimension in both nature and layered manufacturing as well as the interfaces between such. *Chapter 3: Implementation* presents in detail a number of case studies towards enabling 4D printing categorized into the material, time and information dimensions. Two case studies are considered under the material dimension: a variable elasticity rapid prototyping platform and an approach for fabricating variable impedance test

sockets. Towards the time dimension, CNSilk is explored as an on-demand material generation platform. Lastly, Material DNA is discussed as an approach towards linking and embedding information within physical objects. *Chapter 4: Evaluation & Contributions* evaluates the theoretical, methodological and technological contributions of the thesis and *Chapter 5: Conclusions* sums up the work presented and expounds on the future of 4D printing.

2. Approach & Methodology

2.1 Methodology

Much of the inspiration for this research direction stemmed from initial exploration and examination of biological case studies followed by technology surveys to identify key limitations of biomimetic fabrication and rapid prototyping. The work presented in this thesis includes explorations into variable density fabrication (Oxman, Keating, & Tsai, 2011), freeform and tensile member fabrication (Tsai, Firstenberg, Laucks, Sterman, Lehnert, & Oxman, 2012) and digital anisotropy (Oxman, Tsai, & Firstenberg, 2012). The research followed an Analysis-Synthesis-Analysis model where different material systems were first analyzed through imaging as well as chemical and mechanical modeling. Key fabrication characteristics were then incorporated into new processes using both existing and custom-built robotic systems such as the KUKA KR5 sixx R850 industrial 6-axis robotic arm and evaluated. The case studies developed sought to touch on each of the three main categories of the 4th dimension, identified as Material, Time and Information.

2.2 Nature's Way: Biological Parallels for Additive Manufacturing

In Nature, there are numerous case examples of layered construction in material systems across all scales. Unlike machine layered manufacturing systems which typically operate in Cartesian coordinates with material deposition on one plane (e.g. x- y) and layers advancing in the direction of a single axis (e.g. z), Nature employs a much more organic process. The structures that result are products of evolution, which exemplify not only functional design but also principles of the underlying behavior and organization of the process itself (**Figure 1**). Additionally, in Nature, not only do living material systems adapt and fabricate as a result of the environment that they operate in, there is often a propagation of design and information onto other organisms and future generations. Following, we offer a classification of Nature's material systems based on the extent to which they adapt

to environmental conditions and constraints through the modulation of material composition or evolution of form.

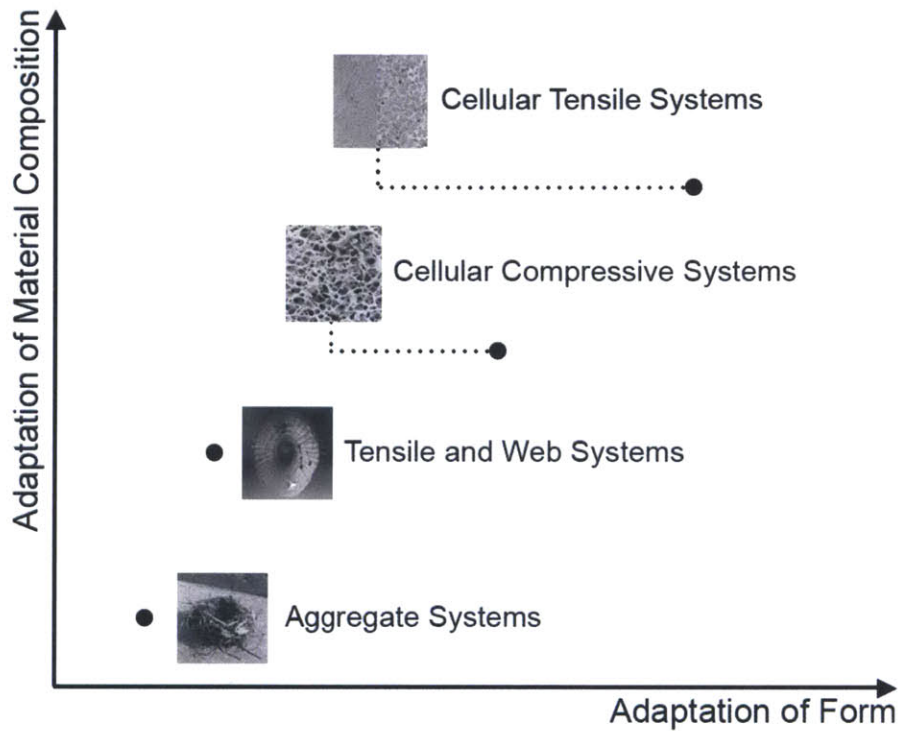


Figure 1. Adaptation of composition and form in Nature's material systems. The material generation process determines, in a way, the extent to which material composition and form may be adapted as a response to environmental conditions and constraints. With aggregate systems such as nests, birds craft with what is readily available in their environment. In cellular compressive systems, e.g. trabecular bone, the density, composition, and hence material properties adapt continuously in response to loading histories.

2.2.1 Aggregate Systems

In aggregate systems, Nature adapts the material system, taking what is available and shaping it according to environmental factors. Many bird species in Nature construct nests of varying complexity through the sculpting, molding, piling, interlocking or weaving of different organic and inorganic materials. The nest designs are, to some extent, inherent to the birds themselves (as different species behave in distinctive manners) but they are also the result of an evolving algorithm

dependent on the properties of the available and chosen materials (Hansell, 2000).

The fabrication process *shapes* the materials as the materials shape the process.

In some ways, complex multifunctional nests speak to the cumulative power of simple design processes and building algorithms. Plain-fronted thornbirds, for example, establish the initial platform for their nests through a long process of carrying sticks to a chosen intersection. Most of these sticks fall until an arrangement is achieved that is sufficient to withstand the wind overnight. The finished nest is a well-designed aggregate of different sticks, grasses, leaves, and other materials gathered from the environment with material distributions informed by function (Thomas, 1983).

2.2.2 Tensile Web and Membrane Systems

In many of Nature's tensile and membrane systems, the material itself is modulated to environmental factors as well as function. Spiders are one of many animals that produce spun fibrous secretions known as silk, which can be arranged into web and membrane structures. Aranaeid spiders, which weave orb-webs, use upwards of seven different types of silks to accomplish different functions (Gosline, Demont, & Denny, 1986). These silks are optimized for a wide range of different conditions, including but not limited to mechanical properties such as strength and toughness. Not only are there different types of silks, but the silks themselves may be rapidly adapted to different parameters during the silk spinning process. The final webs take into account a delicate balance of function, environmental conditions and material efficiency as limited by the energy resources of the spider (Vollrath, 1999).

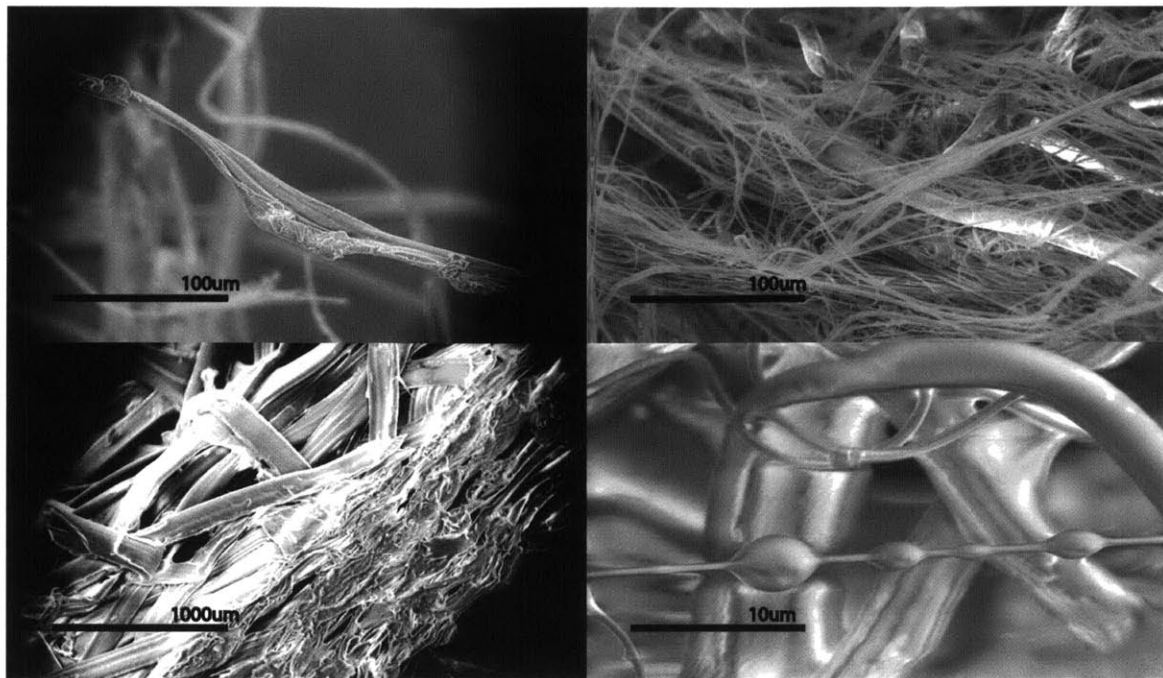


Figure 2. Environmental scanning electron micrographs of spider silk fibers illustrating the different structures present including different fiber widths (top - scale bar 100μm) and droplets of glue (bottom right - scale bar 10μm). Image of cross-section of *Bombyx mori* silkworm cocoon demonstrating fibrous anisotropy and layered construction (bottom left - scale bar 100μm).

The complexity of web systems is further evident in micro and nanostructures observed in silk (**Figure 2**). They are designed not only to respond to immediate factors such as wind, temperature and artifacts, but also to anticipate and predict future events. 3D webs, such as those spun by black widow spiders, are composed of a large number of silk fibers designed to break when struck in order to dissipate the energy required to trap an insect. However, in 2D webs such as orb-webs, the capture threads must not break and hence energy is dissipated through stretching. The molecular structure of these capture threads can be seen as molecular nanosprings, which contribute to its elasticity (Becker, et al., 2003).

2.2.3 Cellular Compressive Systems

In cellular compressive materials systems that develop within living organisms such as bone and wood, a more continuous evolution is evident as loading histories and stresses affect both fabrication and renewal. The structure and density of bone is known to vary depending on the loading conditions that it is subject to (Carter, Fyhrie, & Whalen, 1987). This form is not static, but rather its maintenance and adaptation depends on mechanical forces and loading histories. Bone can be classified as two main types, compact and cancellous, depending on its relative density, with compact bone containing a volume fraction of solids over 70% and cancellous bone under 70%. Cancellous bone is a cellular material that can develop different structures depending on its relative density. At low densities, it forms open cells with rod-like elements; at higher densities, it forms closed-cell structures. These structures are formed as either asymmetric or columnar depending on loading conditions and directions (Gibson, 1985).

The extent of mechanical loading that bones are exposed to is related to the mass and strength of the bones with heavier and stronger bones often observed in heavier individuals (Carter, Fyhrie, & Whalen, 1987). In homeostasis, bone resorption by osteoclasts and bone formation by osteoblasts are equal in rate and hence bone mass and architecture are unaffected. Increased strain in the bone through strenuous exercise for example, may lead to additional bone formation until the new strains are normalized (Huiskes, Ruimerman, van Lenthe, & Janssen, 2000).

2.2.4 Cellular Tensile Systems

Human skin comprises a cellular tensile system with variations in elasticity, stiffness and thickness depending on age, location and function. There is an intelligent predetermination of cellular structure and tensile properties as well as a gradual evolution based on external forces and stresses. Skin tends to be thicker on lower parts of the face compared with upper parts for example (Pellacani & Seidenari, 1999) (Malm, Samman, & Serup, 1995). There's an observed decrease in elasticity with age and increase in thickness in certain locations. These properties

are controlled in part by the microarchitecture of the connective skin tissue and its ability to deform under stress. Modification and impairment of this architecture can lead to improper decreases in elasticity as seen in some pathological skin conditions (Pierard & Pierard, 1977).

2.3 Defining the 4th Dimension

2.3.1 In Nature

Inherent in Nature's material systems are multiple design dimensions, the existences of which are products of both evolution and environmental conditions. These dimensions can be seen as functions of direction, distance or time depending on how they are modulated. Anisotropy in wood grains and animal tissues are often present as functions of direction while material and density gradations in bone and skin are present as functions of distance. Material response, growth, and evolution occur as a function of time over different spans ranging from relatively short nastic movements and tropisms, to adaptation and growth over much longer periods.

2.3.2 In Layered Manufacturing

2.3.2.1 The Material Dimension

In layered manufacturing, each design dimension must be preconceived and deliberate, as form is not yet generated in response to desired functions and necessary constraints. In the material dimension, physical variations of design dimensions as functions of direction and distance may be explored. Traditionally, material properties are assigned discretely to predefined regions during the design and fabrication process of direct rapid prototyping technologies (Sheng, Xi, Chen, Chen, & Song, 2003). When material gradation as functions of distance is considered, variable property gradient printing allows for the creation of systems with tailored material properties designed to complement, enhance and interact with natural systems (Oxman, Keating, & Tsai, 2011).

Anisotropy in natural systems is ubiquitous with most materials exhibiting anisotropic behavior in accordance to their function and behavior. In rapid

prototyping technologies, material anisotropy can be derived from inherent material anisotropy, from artifacts of layered and directional deposition, or from controlled material property gradients (Ahn, Montero, Odell, Roundy, & Wright, 2002) (Cooke, Tomlinson, Burguete, Johns, & Vanard, 2011). Intricate responses may be tailored through computationally determined programmed anisotropy as an approach towards controlled directional material property variation across multiple scales (Oxman, Tsai, & Firstenberg, 2012). Carpal Skin for example (Figure 3), is a process by which hard and soft materials are distributed in a manner where the materials responds to mechanical pressure and forces exerted by the user in a customized fashion (Oxman, Keating, & Tsai, 2011).



Figure 3. Composite image of Carpal Skin, Museum of Science, 2010-2012. Designed by Neri Oxman in collaboration with W. Craig Carter (MIT). 3D printed by Stratasys. Photos: Mikey Siegel.

2.3.2.2 The Time Dimension

Natural material systems are rarely static for the entire duration of their existence. Some systems exhibit adaptive responses directly to stimuli such as tropisms in plants or local skin thickening in areas of stress. Similarly, in layered manufacturing artifacts can be created with functionally graded fabrication approaches.

Also observed in natural material systems are coupled or indirect responses, where external stimuli (e.g. mechanical forces or light) triggers further and perhaps non-directional functionality. Certain varieties of plants, for example, exhibit a variety of nastic movements to stimuli such as light, humidity, contact and temperature. Leaves of the *Mimosa pudica* L. plant undergo seismonastic movements, curling and drooping in response to touch or low levels of light (Fromm & Eschrich, 1988). In layered additive manufacturing, such responses require the development of passive yet dynamic materials capable of accommodating changing functions and environmental conditions. Hierarchical combinations of traditional materials such as polymers and metals with carbon nanotubes (CNTs), for example, may result in breathable facades where pores open and close as governed by the environment (Oxman & Hart, 2008). The ability to print with functional gradients and combinations of responsive materials such as memory-shape polymers holds the potential for the ability to additively manufacture multi-shape objects that can continue to transform after fabrication.

2.3.2.3 The Information Dimension

Beyond physical responses and material variation, systems in Nature enable their perpetuation and evolution through methods of spatiotemporal content variation. On one level, organisms contain DNA, an informational molecule that encodes the genetic instructions for each organism's development and function. Different forms of the molecule in different locations serve different purposes and code for different genes. It may serve as a unique identifier as well as means for

determining the relationships between organisms. This information is not static but is constantly edited in response to environmental factors and mutations. In a similar manner, electronic and chemical information carriers may be introduced in rapid prototyped objects. Examples such as electrically small antennas (Adams, et al., 2011) and micro RFIDs allow for the transmittal and storage of rewritable information within larger objects themselves.

2.4 Interfacing Between Nature and Additive Manufacturing

Nature's design employs complex intricacies and variations in materials and responses inherent across all scales. These different materials and responses fit together with seamless interfaces as a testament to the underlying principles of the behaviors that fabricated them. In human manufacturing, static objects with no variation of function across directions, distances or time fail to capture many of these intricacies. This becomes particularly problematic when considering artifacts designed to function at the interface between objects created by Nature and objects manufactured by man. At the nexus of biomimetic fabrication and additive manufacturing, limitations arise in prototyping with current methods and materials. The use of one or more additional design dimensions, such as material gradation, response and adaptation over time, or controlled volumetric anisotropy in 4D printing offers an approach to addressing this mismatch.

Modeling and Material Representation

The vast majority of commercial modeling, design and analysis software today requires a separate assignment of form and material. The development of freeform surface modeling and the use of nonuniform B-spline (NURBS) mathematics has allowed for the creation of organic surfaces and forms, yet material assignment is still typically homogenous and tied to delineations of form. In additive manufacturing, for example, where the STL file format is widely used, separate files are required for the representation of each material as there is no ability to denote material composition within the file format. Solid objects composed of more than one material must be saved and communicated to a 3D printer as

multiple files. The number of STL files that would be required to represent functional material gradients as found in Nature would be immense and impractical to generate or communicate. Similar concerns towards the need for CAD tools capable of modeling functionally graded material composition have been raised previously in the literature (Jackson, 1999). Section 3.2.3 of this thesis explores the concept of bitmap printing as one potential approach to material gradient representation where a large number of very simple files are generated.

3. Implementation

3.1 Overview

The following sections present a series of explorations into 4D printing as categorized into the material, time and information dimensions. Each dimension is inspired by the biological and delves into particular themes, drawing elements of Nature into the manufacture of the artificial. The material and time sections seek to explore generative platforms and approaches towards enablement of the 4th dimension followed by case studies in the form of specific artifacts. In the case of the information dimension, the example encompasses both.

3.2 The Material Dimension: Direction & Distance

3.2.1 Vision: Adaptation of Composition & Form

Material heterogeneity is omnipresent in Nature and central to determining form relative to function and behavior. Functional material gradients with spatially varying compositions, properties, or microstructures occur across a wide array of biological systems, contributing to material and structural efficiencies at various length scales. In contrast to this, industrially produced items are often homogenous or composed of homogenously defined forms and parts. While such designs are readily compatible with existing manufacturing platforms and design tools, they may sacrifice certain improvements in strength, weight, functionality, and performance.

The material dimension examines the adaptation of composition and form over direction and distance in the design of objects. Digital Anisotropy denotes the strategic control of material property density and directionality in the generation of form and a platform is introduced that seeks to produce digital anisotropy by way of controlled gradients of stiffness and elasticity. Motivated by the disparity in material composition and function observed in interfaces between the human form and manufactured objects, a Variable Impedance Test Socket is designed and fabricated.

3.2.2 Digital Anisotropy: A Variable Elasticity Rapid Prototyping Platform

3.2.2.1 Motivation

In Nature, structures are capable of transitioning seamlessly between different compositions, material properties and microstructures as optimized to specific performance requirements across different length scales. Gradients of elasticity and stiffness in human skin, for example, allow for optimal environmental protection and movement (Agache, Monneur, Leveque, & De Rigal, 1980). Anisotropy is ubiquitous in natural material systems and its modulation in Nature, both locally and globally, is often central to function and structural integrity. An approach, termed Digital Anisotropy, was explored for the controlled density and directionality of material substances in the generation of form allowing for the design of materials and objects, which vary their properties at the micro scale in response to the forces acting on them.

Here, a variable elasticity rapid prototyping platform explores variable property polymer printing in parallel with the addition of limited dynamic responses through the use of a product scale robotic gantry system (Oxman, Tsai, & Firstenberg, 2012). A printing platform capable of mixing and extruding gradient of two materials to fabricate controlled gradients of stiffness and elasticity was built using this system (**Figure 4**). With the ability to create such gradients, products designed to interact with natural systems in a way that complements and enhances their material properties may be fabricated. On a product scale, this may entail wearable artifacts with gradients of stiffness and elasticity that conform to a user through broad ranges of movements. In the future, dynamically controllable elasticity and gradients may be able to respond and adapt as the user shifts through different levels of activity. More broadly, this platform enables the potential to tailor intricate material responses through the fabrication of ‘programmable anisotropy’.

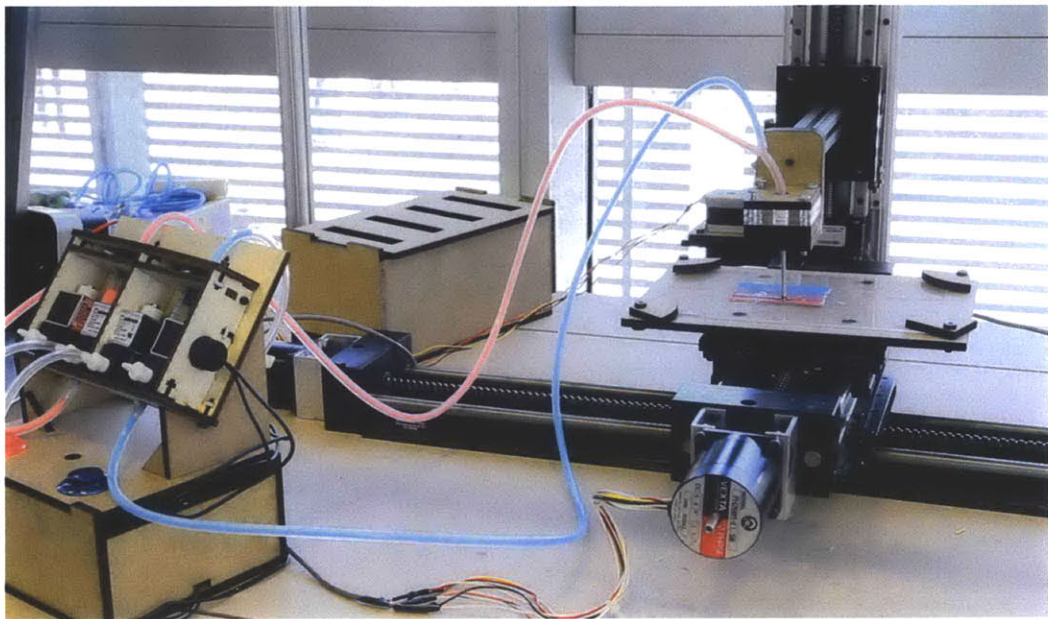


Figure 4. Variable elasticity printing platform with color gradients mapped to different stiffness and elasticity gradients.

3.2.2.2 Design and Control

A printing platform capable of mixing and extruding gradients of two materials was built as an exploration into rapid fabrication with material gradients. A material extrusion head comprising a nozzle and mixing area was attached to the z-axis of a 3-axis gantry robot and a compressed-air driven system was used to control the amount of each material dispensed from its reservoir to the mixing area. Several mixing strategies were explored including diffusive, static, and active mixing.

The platform was designed to extrude materials, which remain liquid at room temperatures prior to mixing and extrusion, and solidify after deposition, i.e. certain epoxies, UV-cure polymers, drying adhesives, and thixotropic fluids. Use of these materials instead of thermoplastics as used in fused deposition modeling printers allows for a larger range of compatible materials. In particular, since the printing process does not require heating the material significantly, the platform is

potentially compatible with temperature-sensitive compounds and biological molecules.

The printing platform was built around a three-axis gantry robot composed of two ball screw linear actuators for the x and y axis and a lead screw linear actuator for the z axis (**Figure 5**). The z-axis actuator was attached to the back of the frame and a horizontal rod was attached to the z-axis to facilitate positioning of the extruder head. Each actuator is powered by a stepper motor. A re-purposed 3-axis CNC motor driver controller with a spindle output is used to control the gantry.

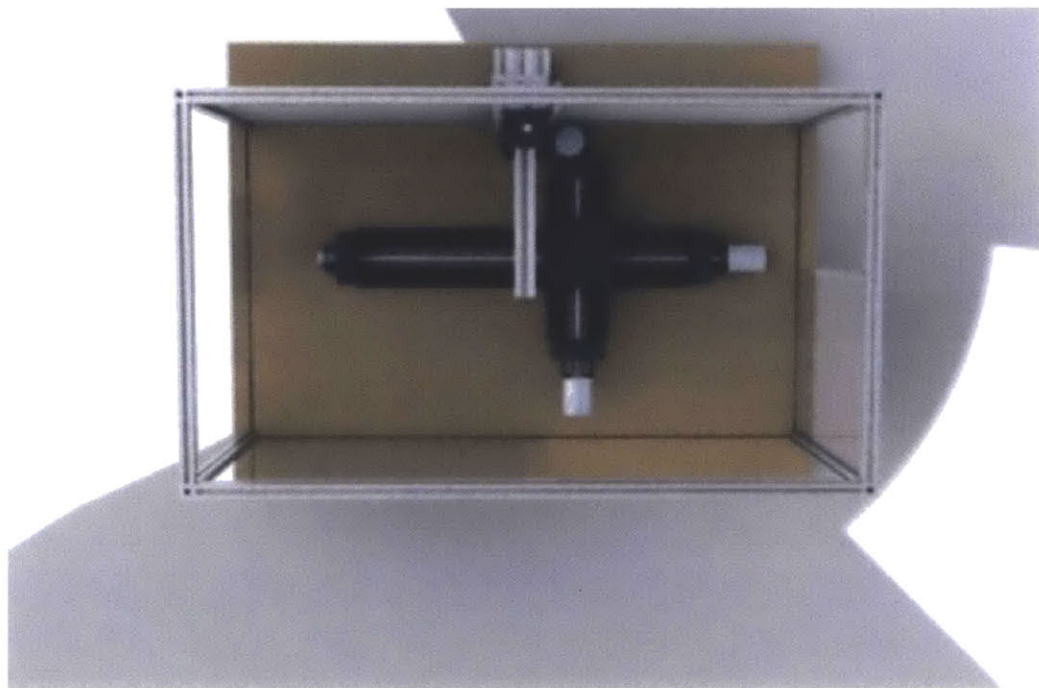


Figure 5. Top view of gantry system model with attached x-y motion stages for actuating the build platform and a separate z-axis with attachment points for the mixer and extruder

The extrusion and mixing system is comprised of material reservoirs connected to pressure sources, a mixing area, and a nozzle (Figure 6). Solenoid valves either switched manually or automatically, were used to control the pressure in the reservoirs and hence the flow rate of material dispensed. From the reservoirs,

the materials are then fed via tubing to a mixing system before being extruded from the nozzle.

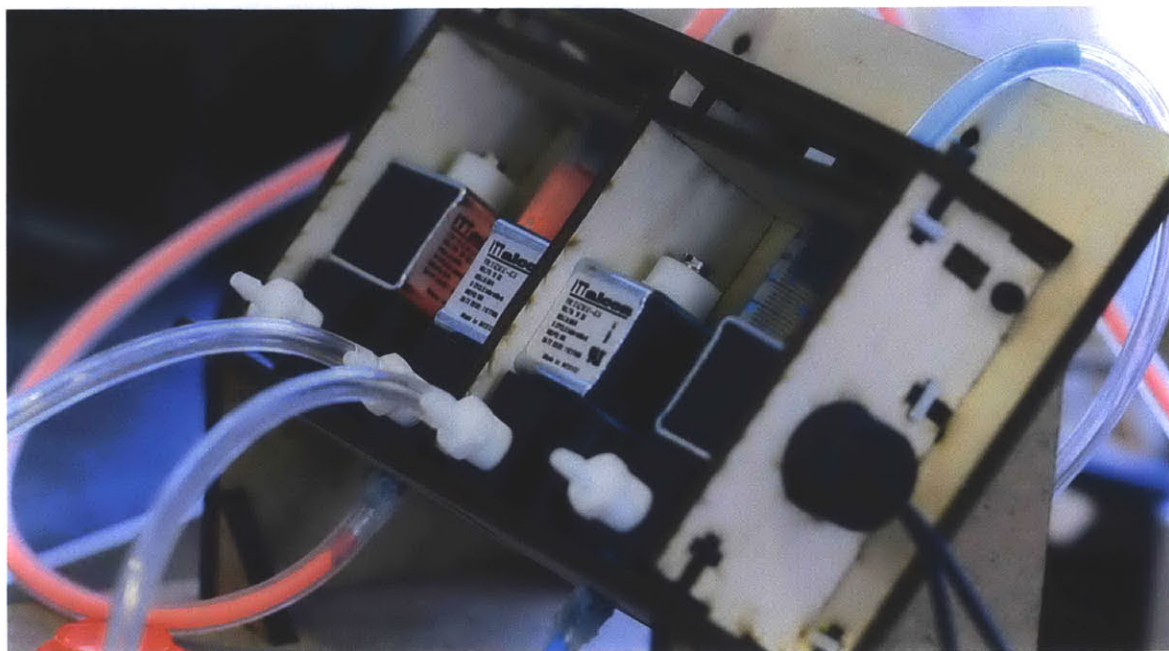


Figure 6. Solenoid valves and material reservoirs. Flow rate of the two materials (shown here in red and blue) were controlled through the actuation of solenoid valves connected to either compressed or atmospheric air. The reservoir and valve assembly may be expanded to accommodate additional materials.

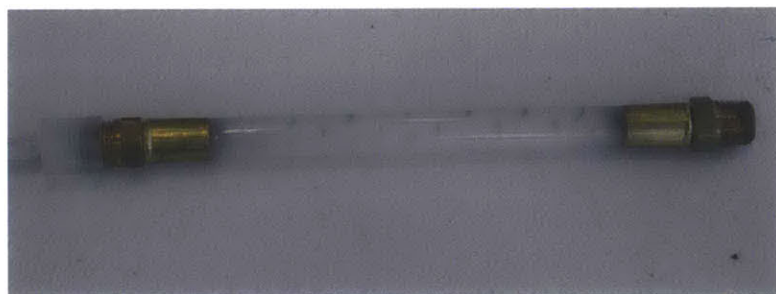


Figure 7. Passive mixer. Static mixers with varying numbers of blade elements were tested and compared to active mixing schemes accomplished by using motorized mixing blades.

Three different mixing strategies were explored: diffusive, static, and active. The diffusive strategy consisted simply of an additional length of tubing between the nozzle and a “Y” connector joining the material feed tubes (see Figure 7). The active mixing strategy utilized a small reservoir immediately before the nozzle into which material could be fed. A set of blades driven by a small motor within the reservoir facilitates mixing. The static mixing strategy used inline static pipe mixers inserted between the nozzle and the material feed tubes.

An aluminum extrusion frame with sliding acrylic doors was designed to enclose the printing platform to provide structure, safety, and environmental control. Additional supports were added to the back of the frame to allow for attachment of the z-axis actuator. The acrylic doors were added in anticipation of working with UV-curable polymers to provide protection from UV radiation. The enclosure that the frame and doors provide also makes it easier to introduce humidity, temperature, and other environmental controls in case more sensitive materials are used.

The gantry platform is controlled using Mach3, a PC-based CNC software. For printing, tool paths were generated from 3D STL models or 2D contour models using PyCam, an open- source tool path generator for 3-axis CNC machining. The resulting GCode is sent to Mach3 and used to control the gantry movement. The viscosity and curing time of the materials being printed are taken into account when setting appropriate line widths.

The material extrusion was separately controlled. The reservoir for each of the materials to be mixed was connected to two valves, one leading to unpressurized atmospheric air and the other to a pressure source. Control of the valves and hence relative amount of each material was provided by a programmed Arduino microcontroller with either preprogrammed sequences or manual control buttons.

In this version of the printing platform, control of material mixing and extrusion was provided separately, and coordinated with the tool path movement to produce the specified gradient. In future versions, the spindle output channel may be used to communicate directly with the extrusion system controller.

3.2.2.3 Gradient Fabrication

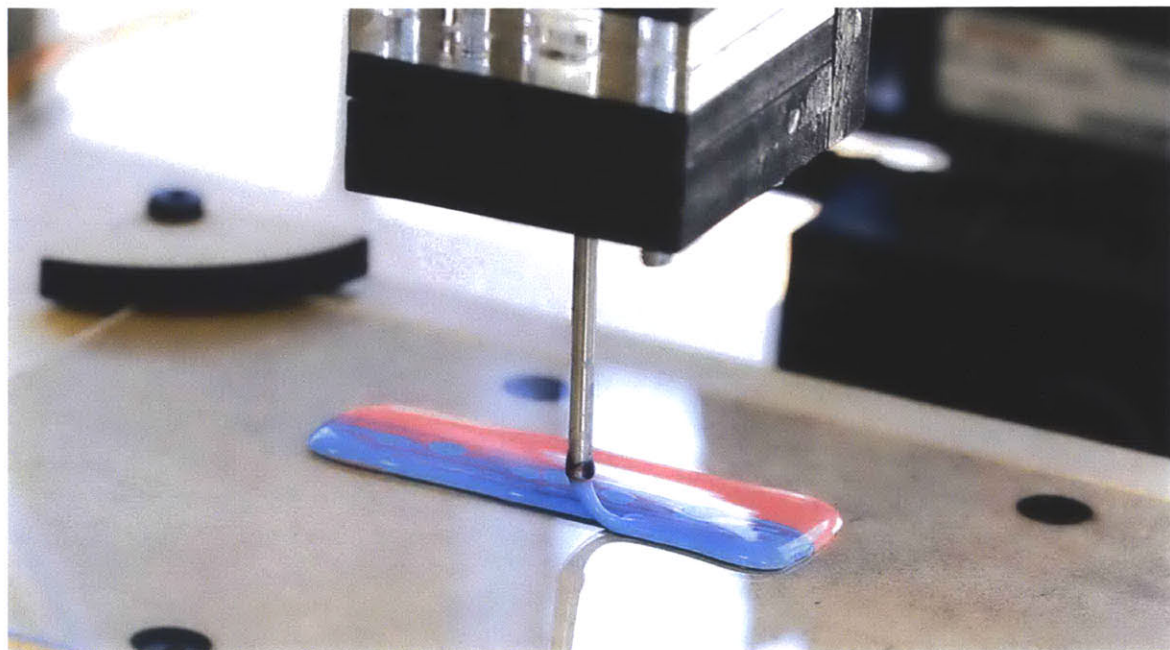


Figure 8. Color gradients being created on the 3D printed platform by mixing red and blue adhesives in different controlled ratios.

In Figure 8, the platform is shown printing with blue and red glue. The two adhesives are mixed in different ratios to produce varying color gradients. The cast sheet in **Figure 9** demonstrates a similar principle, where a softer blue-colored silicone (Shore 00-10) is mixed with a harder red-colored silicone (Shore 00-50) to produce gradients in both color and durometer. Other combinations of materials tested for potential use on the platform include UV cure silicones and polyurethanes as shown in **Figure 10**. In the future, ratios of aggregates, foaming agents, or responsive materials may also be introduced.



Figure 9. Cast silicone sheet where a softer blue-colored silicone (Shore 00-10) is mixed with a harder red-colored silicone (Shore 00-50) to produce gradients in both color and durometer.

For the adhesive used in the printer, passive mixing was sufficient to create color gradients. The inline static pipe mixers produced the most complete mixing with the smoothest gradients, however, the fluid flow and fill patterns in the mixers combined with the substantial length of the mixers (0.1905m to 0.2437m) made it difficult to control and change gradients quickly. The diffusive mixing strategy enabled adequate gradient production and rapid changes in gradient composition. The nozzle used in the current prototype was chosen from an assortment of stainless steel dispensing needles ranging from 7 gauge to 14 gauge, depending on the extrusion line thickness desired. For the fairly low viscosity and long drying time of the adhesive used, a 10 gauge needle was used.

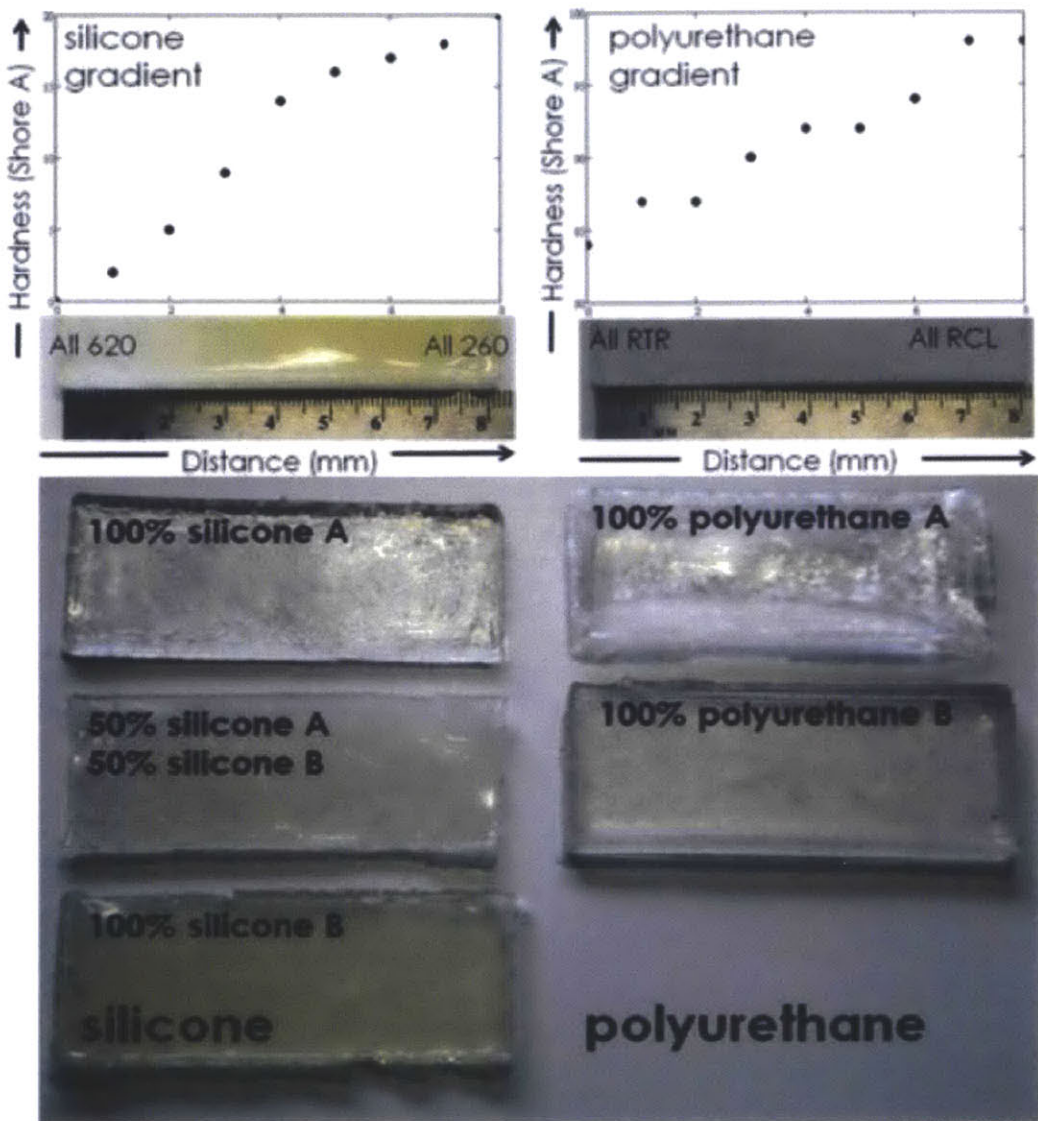


Figure 10. UV cure silicone and polyurethane samples tested. A series of samples were made by combining UV curable silicones and polyurethanes with different shore values in a gradient across each sample. (Oxman, Keating, & Tsai, 2011)

While adequate for demonstrating variable property gradient printing, the gradient mixing strategies presented thus far are difficult to control and use a relatively large volume for mixing. In parallel to the development of the printer, several other gradient creation mechanisms are being explored. One method seeks

to generate controlled two-dimensional gradients prior to extrusion (**Figure 11**) rather than the 1 dimensional gradients produced by the current printer.



Figure 11. Two-dimensional gradients generated in a microfluidic device using red and blue dyes. The geometry of the gradient is controlled by tuning the flow rates and pressures of multiple flow streams (Oxman, Tsai, & Firstenberg, 2012)

3.2.3 Physical Interfaces: Variable Impedance Test Socket

3.2.3.1 Motivation & Background

Prosthetic socket comfort and quality affects the ability of a patient to use his or her prosthesis and plays a role in preventing the development of future pathological conditions. Unlike standardized prosthetic components such as knees or ankle-foot prostheses, prosthetic sockets are typically custom fabricated for each patient by individual prosthetists. The process of making such sockets, undertaken by a prosthetist, is labor intensive and iterative and can take several weeks to complete (Klasson, 1995). Incorrect socket attachments may cause sores and other discomforts in an amputee's daily routine (Johannesson, Larsson, & Oberg, 2004).

In stark contrast to the complex physiology of a residual limb, the resulting socket is typically composed of a homogenously rigid material. As the shape and volume of a residual limb can fluctuate during each step and between different levels of activity due to muscle contractions and other forces, there is a desire for sockets to be able to comfortably accommodate a broad range of movements (Sanders, Harrison, Allyn, & Myers, 2009) (Staker, Ryan, & LaBat, 2009).

Although computer-aided design and computer-aided manufacturing (CAD/CAM) tools are available, the design and fabrication of a functional socket still remains largely an art. Quantitative anthropomorphic data collected via internal and surface image capturing technologies such as MRI, CT and ultrasound can provide some insight into tissue distribution within the residual limb. Here, residual limb stiffness plays a key role in scientifically determining final socket shape and material stiffness. Prior research suggests that there is an inverse relationship between residual limb stiffness and socket pressure along the socket- residual limb interface. For example, areas of the limb with boney protuberances require softer interfaces while softer tissues may be able to interface with stiffer materials.

Using spatiotemporal stiffness data collected about a residual limb, a process for the design and fabrication of a Variable Impedance Test Socket (VTS) is explored. A mapping of collected limb data to appropriate socket structures and materials is used to inform design for the rapid prototyping and fabrication of a VTS.

Related Work

The concept of using softer materials in contact with support for boney protuberances and harder materials to support higher loads of softer tissues has been previously explored in socket technology through the use of “windowing.” (Sewell, Noroozi, Vinney, & Andrews, 2000) This windowing approach however, is coarse and fails to provide a necessary level of spatial control of dynamics. Another similarly coarse approach seeks to achieve distinct areas of mechanical response by assembling multiple parts composed of different materials (Laferrier & Gailey, 2010).

Conventional fabrication of prosthetic sockets are produced using a individually customized artisan process. More recently there has been research interest in automated socket fabrication via rapid prototyping. Sockets produced in this way tend to be composed of hard polymers such as ABS and homogenous in composition (Herbert, Simpson, Spence, & Ion, 2005). As part of his master’s thesis,

David Sengeh (Biomechatronics Group, MIT Media Lab) produced a multi-material 3D printed socket using Objet's Connex500 polyjet technology (Sengeh, 2012). This proposal seeks to produce a VTS that is further informed by ATS data and contains much higher resolutions in material and structural motif mapping.

There have been some research investigations into correlations between residual limb stiffness and ideal socket shape. These typically suggest that there is an inverse relationship between residual limb stiffness and localized socket pressures (Sanders J. D., 1993) (Silver-Thorn, Steege, & Childress, 1996) (Mak, Liu, & Lee, 1994). This may allow the determination of ideal socket shapes by optimizing the maximum socket pressures when bearing the weight of the amputee using the residual limb stiffness distribution measured by the ATS.

3.2.3.2 Process Overview

In conventional carbon fiber sockets, pressure distribution within the socket is controlled through areas of compression, contact and voids. More recent technologies achieve varying degrees of compliance over certain anatomical features through changing socket wall thickness or adding mechanical features. "Windowing" techniques where patches of softer materials are added to a socket provides some variation of socket compliance over the residual limb but lack the necessary spatial control of dynamics to ensure a comfortable interface.

Fabricated using a Stratasys Objet500 Connex 3D printer, the Variable-Impedance Test Socket (VTS) is designed using data collected about a residual limb (**Figure 12**). Taken over the entire limb, the data may be used to calculate the linear, first-order stiffness of the tissue at each given point (Phillip & Johnson, 1981). The inner shape of the VTS socket is computationally determined from this data and the wall stiffness of the VTS is inversely proportional to the tissue stiffness measured. The VTS is passive and relatively lightweight allowing for dynamic testing under typical use conditions in a prosthetics facility.

The commercially sold Stratasys Objet500 Connex 3D printer and its affiliated software are capable of working with fourteen Digital Materials with a range of elastic modulus and durometer. The high resolution of the printer (600 dpi in X, 300 dpi in Y and 845 dpi in Z) allows for a high spatial resolution of material to tissue stiffness gradient matching. Smooth transitions between hard and soft materials can be designed, avoiding the edges and hard transitions seen in windowing techniques. The socket is printed layer-by-layer in the Z direction and all materials are incorporated in one process.

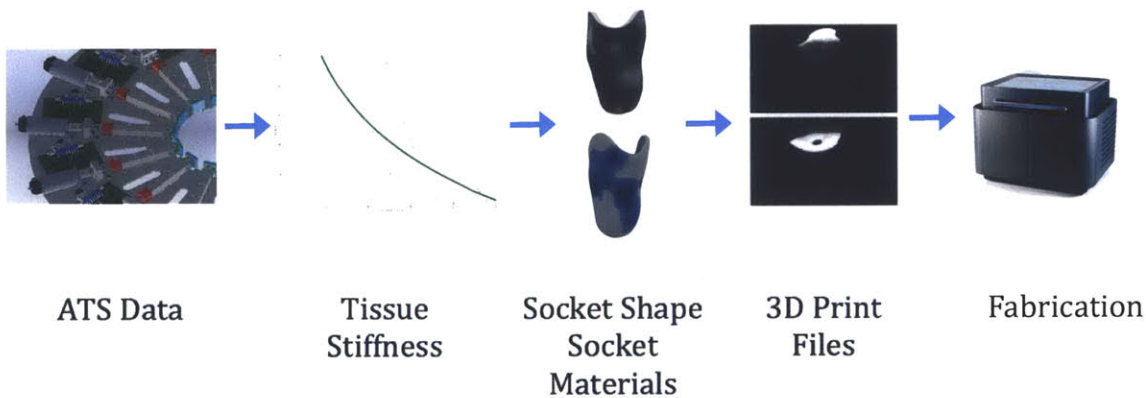


Figure 12. The VTS design and fabrication process begins with data collected on a residual limb, including local tissue stiffness. This data may be derived from MRI scans or using an Actuated Test Socket (ATS) and is then used to computationally generate socket shape and socket material distribution. The socket shape and material distribution are incorporated into bitmaps or STL files that are then sent to a 3D printer for fabrication.

If quantitative feedback is required, especially with regard to peak pressures over anatomical features of interest, off-the-shelf solutions may be employed, for example the Tekscan F-Socket Pressure Analysis System. Ongoing work in this direction is exploring the feasibility of incorporating 3D printed optical sensors into the current fabrication process of the VTS. Such sensors may be able to provide real-time feedback on socket wall deformation, shear stresses and pressure.

3.2.3.3 Data Collection

ATS Data

In the final system, data will be collected physically using the ATS as developed by Arthur Petron (Biomechatronics Group, MIT Media Lab). The socket shape under load in real time, the pressure response at different tissue displacements and the local impedance of residual limb tissue may be measured. From these measurements, the local nonlinear first order stiffness at each location on the residual limb will be passed on to the VTS generation process.

Test Data

Since the ATS and VTS development tracks were scheduled to run in parallel, a set of realistic test data was constructed to allow data to socket structure and material mapping to commence. Test data was derived from three sets of data taken from the same residual limb: an MRI scan of the limb encased within a silicone liner, Tekscan F- Socket pressure distribution along the socket-limb interface under unloaded positions, and 3D scan data of the inner surface of an existing, well-fitting carbon fiber composite socket for the limb.

3D representations of the residual limb were reconstructed from MRI images using the Mimics Innovation Suite software package developed by Materialise. Radial tissue thickness at each point on the limb was measured using the 3-matic software sub-package. Tissue thickness here is defined as the horizontal radial distance between the surface of the skin and the underlying bone.

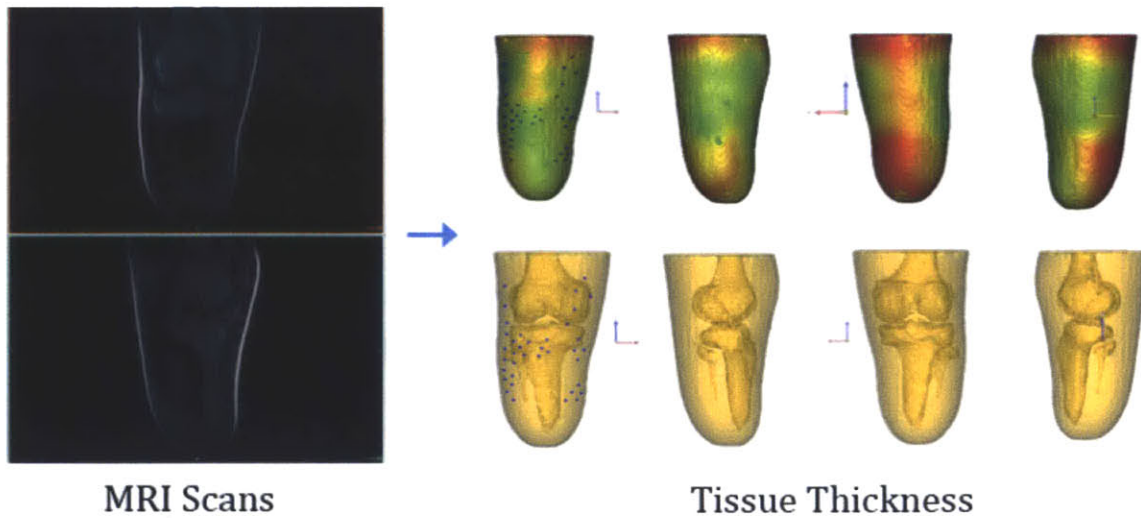


Figure 13. (Left) Images from MRI scan of a right residual limb as seen in Mimics. (Right - top) Representation of tissue thickness in the residual limb with areas of high tissue thickness denoted in red. Views from left to right are anterior, lateral, posterior, medial. (Right – bottom) 3D reconstruction of residual limb bone and tissue in 3-matic. The blue dots on the anterior view denote the points selected for K-value calculations. (Tsai & Oxman, 2013)

The 3D scan surface data from the existing carbon fiber socket was also imported into Mimics and the horizontal radial gap between the socket and the residual limb surface was measured using 3-matic. This distance is referred to in the following passages as “tissue displacement” (**Figure 13**)

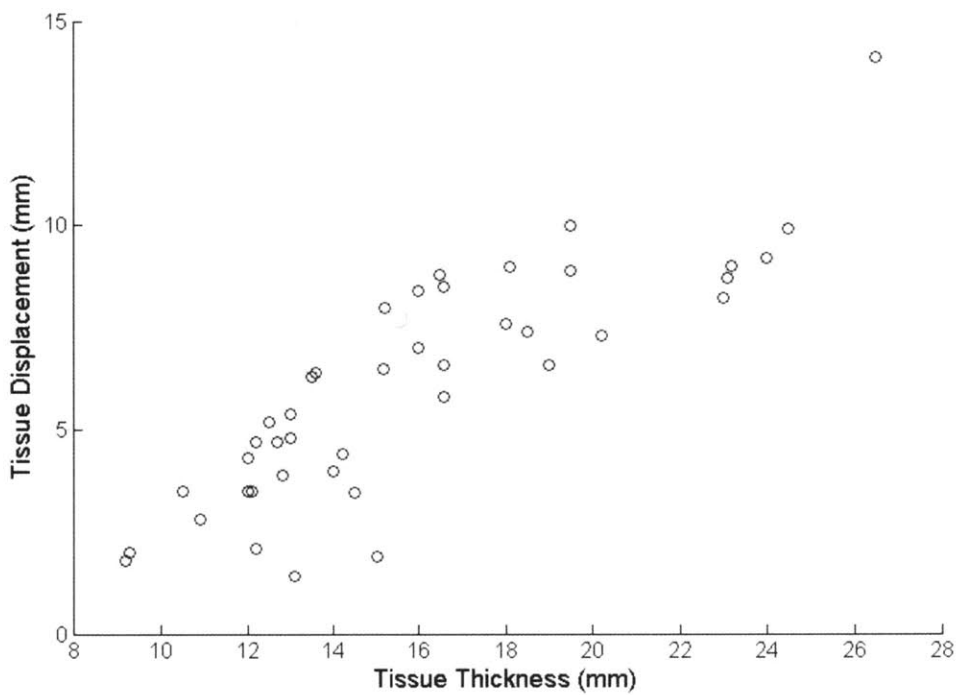


Figure 14. Tissue Displacement VS Tissue Thickness for points along the tibial crest and femoral condyles.

Pressure data from the Tekscan F-socket system in the form of tab-separated text files were opened in Excel. Normal forces at these points were derived by dividing the pressures over the measurement area. Several points as seen in **Figure 14**, particularly over anatomical areas of interest such as over the tibial crest and along the femoral condyles were selected. Stiffness values (K) at these areas were calculated using the force (F) and tissue displacement (R) data using Hooke's law $K = F/(R)$. The best-fit equation for these values was estimated to be $K = -141.6 \ln(R) + 462.8$ using Matlab (**Figure 15**).

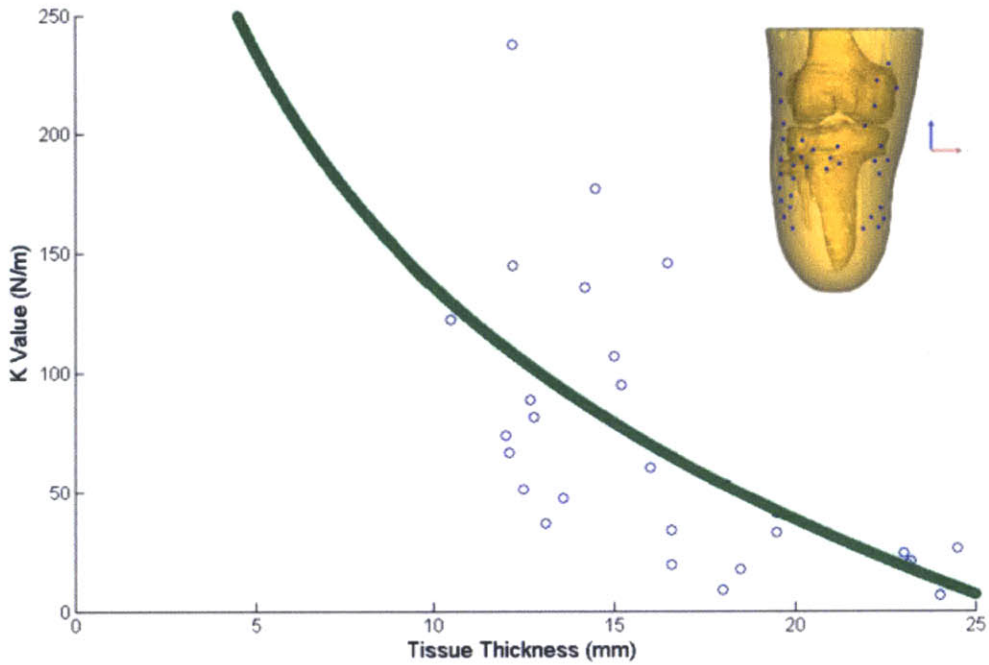


Figure 15. Stiffness VS Tissue Thickness for points along the tibial crest and femoral condyles as indicated by the figure in the upper right.

Data Structure

The data structure for communication between the ATS and VTS generation method is a tab delimited text file with columns for *plateID*, θ , *r*, *z*, *F* and *t*. *PlateID* denotes the ATS actuator ID the measurement was taken using; θ , *r* and *z* are the coordinates of where the data was taken in degrees and mm (**Figure 16**); *F* (N) is the force used; and *t* is the time in seconds from the beginning of the measurement sequence. The test data set was written using the same structure with null values for *plateID* and *t*.

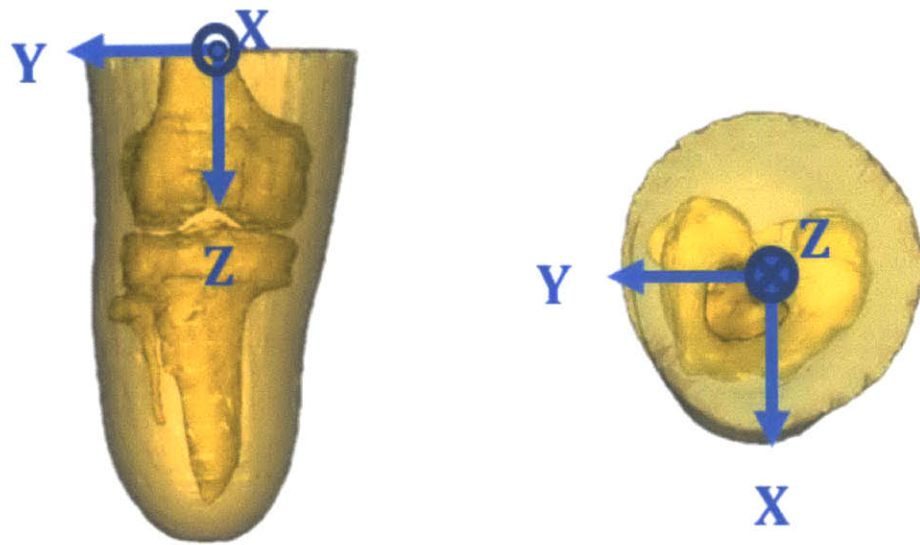


Figure 16. Origin and axis for data structure. The origin is taken to be the center of the limb at a height equal to the top of the future socket cut lines as determined by a prosthetist. θ increases clockwise from the center of the patella when viewed from the top. (Left) Anterior view. (Right) Top view.

3.2.3.4 Modeling

The ability to accurately model the biomechanics of the soft tissues of a residual limb is important in understanding the dynamic interaction between the limb and the socket and should play a role in informing future designs of both the VTS and potential active sockets and interfaces. The properties of skin depend primarily on the interactions of dermal collagen and elastic fiber networks within the ground tissue matrix with some contributions from the epidermis (Chen, 2008). At small displacements, the behavior is roughly linear elastic as the elastin and reticular fiber matrix deforms. At larger deformations, tissues experience strain hardening and there is a static nonlinearity that scales with depth into the tissue (Elsner, Berardesca, & Wilhelm, 2002).

When considering *in vivo* indentation testing as is the case with the ATS, there are several additional issues that arise including the effects of Langer's lines,

muscularity, and isotropy in fleshy areas (e.g. the posterior compartment of the leg) and contributions to stiffness from bone in areas of thin tissue thickness (Hayes, Keer, Hermann, & Mockros, 1972). In the analysis done in section 3.2.3.3 above using the test data set constructed from MRI images, a simple linear elastic material model is used to approximate stiffness values at each point. There is some basis in the literature for this as linear properties typically contribute the largest role towards daily physiological stress levels (BIschoff, Arruda, & Grosh, 2000). In reality however, soft tissues typically have non-linear stress-strain and viscoelastic behaviors, calling for geometrically non-linear approaches (Doblare & Garcia-Aznar, 2008).

In this section, a number of commonly used hyperelastic and viscoelastic material models are presented and discussed in view of suitability towards fitting experimental ATS data.

Material Models for Biological Tissues

Hyperelastic materials are ideally elastic materials for which there exists a strain energy density function W , the derivative of which in respect to a strain component ε is the stress component S . The hyperelastic idealization assumes a stress-strain relationship that is non-linearly elastic, incompressible, isotropic and more or less independent of strain rate. Hyperelastic assumptions are generally suitable for pseudoelastic tissues and widely used models include the Neo-Hookean, Mooney-Rivlin, Ogden and Arruda-Boyce models (Xu, Teoh, & Sun, 2002) (Weiss, Gardiner, & Quapp, 1995).

Mooney-Rivlin and Ogden are two of the most commonly used phenomenological models for biological tissues. Mooney-Rivlin is generally suitable for strains up to 200% and Ogden up to 700% (Mooney, 1940) (Ogden, Non-Linear Elastic Deformations, 1984). For certain material constants and strain invariant constraints, the 6-parameter Ogden model simplifies to the 2-parameter Mooney-Rivlin model. For both empirical methods, multiple modes of mechanical testing are

recommended and results may not be as robust as those of mechanistic models (Korochkina, Claypole, & Gethin, 2005) (Ogden, Saccomandi, & Sagura, 2004).

The Neo-Hookean and Arruda-Boyce models are mechanistic models derived from the statistical thermodynamics of cross-linked polymer chains and 8-chain networks within a representational volume, respectively. For small displacements, the Arruda-Boyce model reduces to the Neo-Hookean model. Based on its underlying cross-linked polymer framework, the Neo-Hookean model is typically only accurate at lower strains (< 20%) (Treloar, 1948) (Arruda & Boyce, 1993). The Arruda-Boyce model on the other hand is generally accurate up to strains of 300% when used to describe rubbers and polymeric materials. Compared to the empirical Mooney-Rivlin and Ogden models, the mechanistic models deliver decent curve fits even with limited experimental data and typically provide reasonable approximations of behavior in other modes of measurement (e.g. prediction of behavior under uniaxial tension using data collected from equibiaxial tensile testing) (Marlow, 2003).

When considering the dynamic response of biological tissues, it becomes apparent that it may be beneficial to model the frequency-dependent system response. There are three typical viscoelastic solid material models that have been investigated extensively with regard to biological tissues in the literature: Maxwell, Kelvin and Voigt (Elsner, Berardesca, & Wilhelm, 2002). When a high degree of modeling accuracy is desired, hybrid hyperelastic linear or nonlinear viscoelastic models may also be constructed (Weiss, Gardiner, & Quapp, 1995) (Xu, Teoh, & Sun, 2002). These systems allow for the modeling of behaviors such as creep, hysteresis and stress-relaxation, which may be useful when considering the design of active prosthetic sockets, which may change in stiffness or geometry to accommodate different modes of use.

In the case of data taken using the ATS, precise unperturbed tissue thickness (radial from the surface of the skin to the surface of the underlying bone) and hence the strain will be difficult to obtain given the *in vivo* nature of the measurements.

Future analysis would benefit greatly from experimental measurements or MRI-based estimates of tissue thickness at each point of indentation. As the ATS is designed to take only uniaxial compressive measurements, mechanistic models such as the Arruda-Boyce model may be more useful for predicting behavior in response to tensile or shear forces.

3.2.3.5 Material Mapping

For this initial round of testing and fabrication, tissue stiffness was mapped to material hardness using an inverse relationship. Stiffness ranges are given in Table 1 below. Objet Digital Materials are produced by combining two compatible materials – one hard and one soft - in specific proportions. Renderings of the resulting socket using this material mapping is shown in **Figure 1**.

Table 1. *Objet Digital Materials and durometer for tissue stiffness K values. Locations with a K Value below 65 N/m were mapped to one of the hard Objet Digital Materials. Data taken from www.objet.com*

K Value (N/m)	Objet Digital Material ID	Digital Material Durometer (Shore A)
125 - Max	FLX930	27
100 - 125	FLX 9040-DM FLX9940-DM	37.5
85 - 100	FLX9050-DM FLX9950-DM	47.5
80 - 85	FLX9060-DM FLX9960-DM	60
75 - 80	FLX9070-DM FLX9970-DM	70
70 - 75	FLX9085-DM FLX9985-DM	82.5
65 - 70	FLX9095-DM FLX9995-DM	93.5

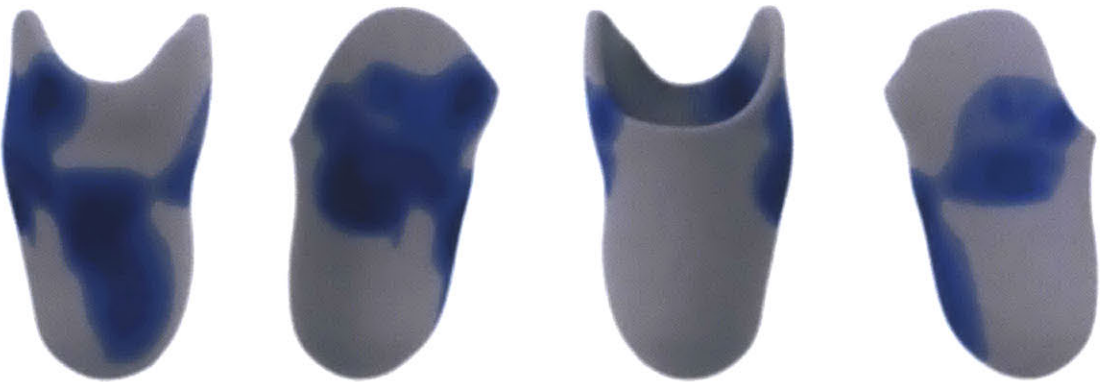


Figure 17. Rendering of the VTS (right limb) with grey representing areas of the socket mapped to hard Objet Digital Materials and blue representing areas of the socket mapped to soft Objet Digital Materials. Softer materials are represented by darker shades of blue. (Left to Right: anterior, lateral, posterior, medial views). Renderings by E.L. Doubrovski.

3.2.3.6 Shape Determination

The shape of the socket was derived from considering the pressure balance between the force from the body and the forces between the residual limb and the socket (**Figure 18**). The force (F_{top}) from the body was taken to be equal to half the weight ($W/2$) of the user. A cross sectional area (A) was estimated as the area of the disk across the residual limb at the top of the socket and the pressure (P) was calculated as $P = F_{top} / A$. The force (F_{inner}) at each point of inner socket surface was then calculated as $F_{inner} = P/dA$. Using the tissue stiffness K values estimated previously at each point, the radial displacement (Δr) of the inner socket wall relative to the residual limb surface was calculated using Hooke's law $\Delta r = F_{inner} / K$. All calculations were done using Matlab or PyLab.

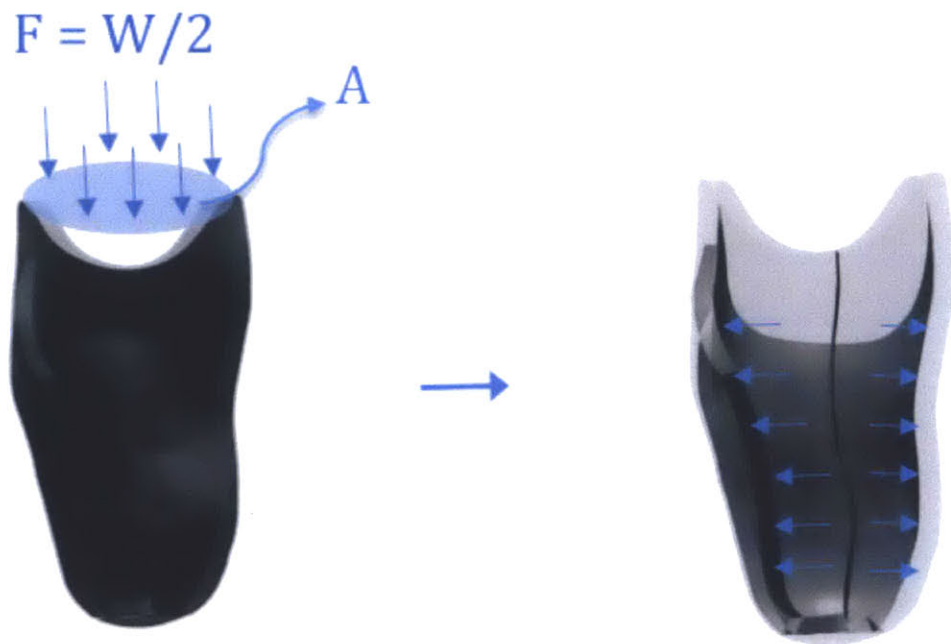


Figure 18. Determining socket shape by assuming equal pressure distribution along the inner socket surface and using K values.

Because a patellar-tendon-bearing socket was desired for this particular test subject, socket geometry from the existing carbon-fiber socket was used to create an indentation in the patellar-tendon region (Convery & Buis, 1998). In addition, the socket cut lines created by a prosthetist in the existing socket were used as guides to determine the cut line geometry in the VTS design. The final data set prior to file generation contains the following columns $plateID$, θ , r , z , F , t , K , $MatID$, Δr , and $rnew$, where $MatID$ denotes the Objet Digital Material mapped to the tissue stiffness (K) and $rnew = r - \Delta r$.

3.2.3.7 File Generation

Following the mapping of materials and socket geometry, files were generated for the 3D printer. Typically, files generated for the Objet Connex500 are loaded into the Objet software in the form of STL files with an individual file for each

material. Given the high resolution of our material mapping and the desire to generate smooth transitions between materials of different hardness and avoid sharp edges of transition between hard and soft materials, the VTS is fabricated using a method termed “bitmap printing”.

In bitmap printing, binary bitmap files are written which indicate to the printer where drops of each material should be jetted. The Connex500 prints in layers normal to the print bed (the Z axis) with a resolution of 845 dpi. An object similar to a VTS with a height of approximately 5 inches is hence split into around 4225 layers. Each layer in the Z direction requires a separate set of 2 X-by-Y bitmaps. These files – and hence control over the drops of materials jetted – are written at the resolution of the printer (600 by 300 dpi – X by Y). The percentage of each material patterned at this scale determines the overall hardness of each larger region. Support material is jetted for voids where there are additional areas of the socket specified above it. For example, when the VTS is printed on its side, support material is printed to fill the inside of the socket. For these initial trials, scripts were written in Matlab and Python to generate bitmap files.

Compared to the high resolution of the printer and hence the bitmap files required (600 by 300 by 845 dpi – X by Y by Z), stiffness data on the residual limb is relatively sparse. Initial attempts to map directly from material stiffness and geometry in the data set to bitmaps resulted in gaps and pixilation. The strategy employed below first reconstructs a STL mesh from the final data set and then maps between *MatID* in the final data set and binary bitmap images of slices of the STL.

STL Mesh Reconstruction

To create a solid STL of the VTS, θ , r and z columns from the final data set were exported and converted to a 3-tuple point cloud file with Cartesian x, y, z coordinates. MeshLab V1.3.2 was used to perform the mesh surface reconstruction – note that this surface corresponds to the inner surface of the VTS. This STL surface reconstruction was then lofted out 15 mm to create a solid STL of the VTS geometry.

The distance of the loft may be altered depending on the desired thickness of the VTS.

STL Slicing & File Generation

The STL of the VTS is sliced into a set of M binary bitmap images of dimension p -by- q at thicknesses corresponding to the Z resolution (845 dpi) of the Objet500 Connex. A material data set is constructed composed of x , y , z and $MatID$ values from the final data set. The material data set is divided into M sub data sets by z value corresponding to the slice height. Each sub data set is mapped onto a p -by- q image array with $MatID$ values as the entries. The Euclidean distance and nearest-neighbor transforms are computed for each array.

For every point in each STL slice that belongs within the socket, an $AvgMatID$ is calculated by the distance weighted average of the $MatIDs$ of the nearest three points in space. The result is a set of M image arrays composed of 0s for each point not in the socket and $AvgMatID$ values for each point within the socket.

The set of M image arrays containing $AvgMatID$ values are then scaled and smoothed to fit the 600 by 300 xy resolution required by the printer. Two binary bitmap files are written for each $AvgMatID$ image array, one for each of the two Digital Materials used by the printer. Generally, a value of 1 results in material deposition and a value of 0 results in no deposition, with the exception of support material, which is deposited at positions where both files read 0, but further build material is expected above. At any index position, the values of the two files may not both be 1.

The distribution density of each material at the resolution limit determines the mechanical characteristics (e.g. stiffness) of the object on the macroscale. As discussed in section 3.2.3.5, each $AvgMatID$ value is assigned a relative proportion of one material to the other (e.g. a value of 10 is mapped to 1:1 of material A to material B). Here, the presence (a value of 1 or 0 in the bitmap) of material A, for example, is randomly decided by a probability distribution function weighted

according to *AvgMatID*. An example of a set of bitmaps for a given layer is shown in *Figure 19*.

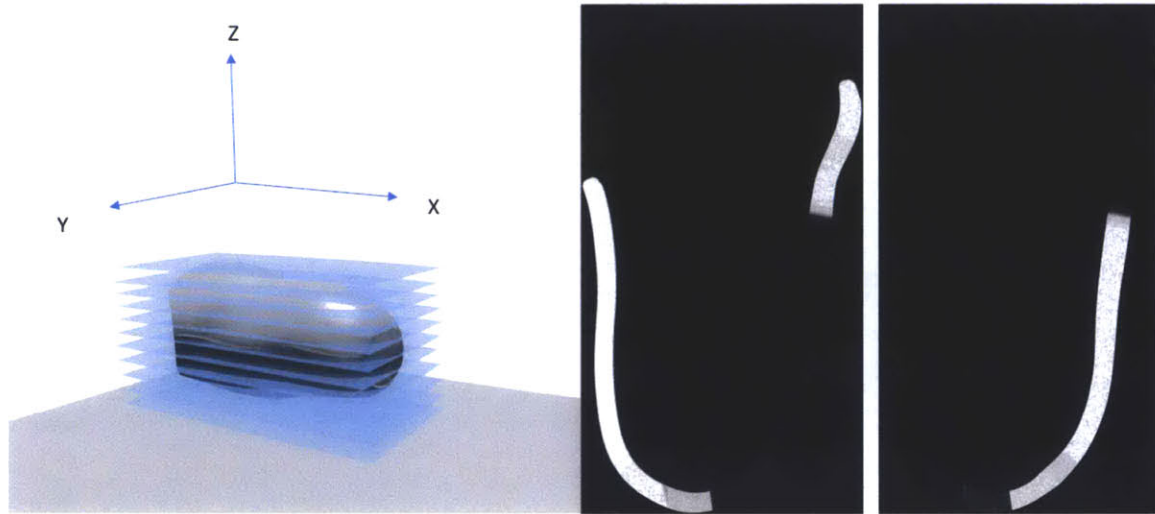


Figure 19 (Left) The socket STL was sliced horizontally, each slice corresponding to a layer of material deposition by the printer. Each slice is then written as two bitmap files (right), one file per material.

3.2.3.8 Socket Fabrication

The VTS is printed using the Stratasys Objet500 Connex. The longest dimension is set along the z axis and the shortest axis is set along the z axis to minimize the number of bitmap files needed and the print time. For a VTS with dimensions of approximately 8.5 by 5.25 by 5 inches, the estimated print time is around 25 hours. The printed socket using clear VeroClear and black, opaque TangoBlack is shown in **Figure 20**.

Although 3D printing with Digital Materials allows for an unprecedented amount of freedom in geometries and the number of materials that can be fabricated in one process, they are not structural enough to support the weight of an average human over any prolonged period unless the socket thickness is made to be extremely large (e.g. in excess of 1 inch.) To ensure testing safety and avoid the need for a very thick and heavy socket, a composite carbon fiber shell is made to fit

outside the 3D printed layer. A standard male pyramid is used as the attachment between the composite carbon fiber shell and prosthetic pylon.



Figure 20. Variable impedance transtibial prosthetic socket bitmap-printed using the Stratasys Objet500 Connex. The darker areas contain higher percentages of the soft rubber-like Tango Black Plus and lighter areas more of the rigid, transparent Vero Clear material. This socket was written on 8832 bitmap files corresponding to 4416 slices and material deposition layers. (Tsai & Oxman, 2013)

First Composite Shell

The geometry of the outer composite shell is similar to that of the outside of the 3D printed layer. Gaps between the outer shell and the 3D printed layer are incorporated in order to allow soft areas of the 3D printed layer (i.e. along the tibial crest) to deflect outwards when loaded (**Figure 21**). The size of the gaps were designed to be proportional to the softness of the neighboring 3D printed layer material with a gap of 5.5mm between the outer shell and the softest printed materials and no gap between the outer shell and the hardest printed materials. An STL of the outer composite shell was created using Meshlab from data calculated in Matlab. A 2-part female mold was CNC milled out of polyurethane foam from which a female plaster of paris mold was cast. A certified prosthetist fabricated the composite shell using conventional socket fabrication techniques.

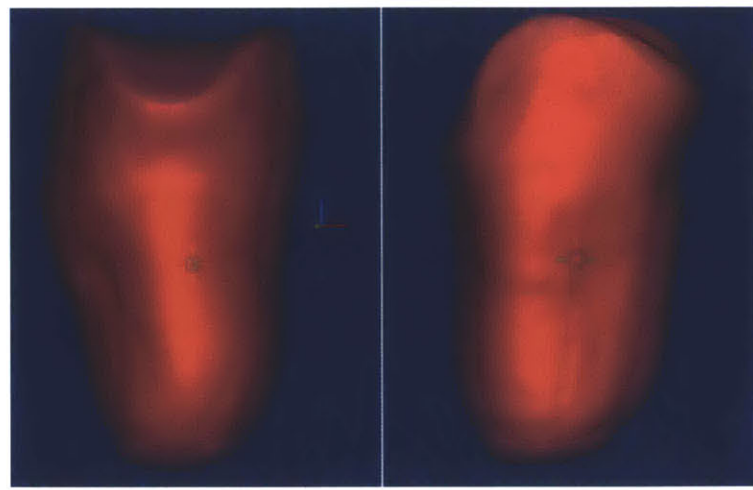


Figure 21. Renderings in Mimics showing the spacing between the inner surface of the 10mm thick 3D printed layer and the inner surface of the outer composite shell. (Left) Anterior view. (Right) Lateral view.

Second Composite Shell



Figure 22. Vacuum bagged layup of second composite carbon fiber socket shell.

Following the printing of the VTS on the Objet500 Connex, a second composite shell was fabricated. A female mold of the exterior of the VTS was cast using Smooth-On Ecoflex 00-30. Plaster was poured into the female mold to create a male mold used as the base of the carbon fiber layup. Two layers of a 6-inch diameter braided carbon biaxial sleeve and System 2000 Epoxy Resin with 2060 Epoxy Hardener from Fiber Glast were used to create the final layup (Figure 22).

3.3 The Time Dimension: Growth and Response

3.3.1 Vision: Fabrication Material Behavior & Response

Material systems in Nature can perhaps best be characterized by growth, adaptation and adaptation through growth. These characteristics extend beyond synthesized biological specimens to material generation during the very process of growth and fabrication. Loading patterns affect bone structure; weather conditions influence the architecture of spider webs; touch causes the leaves of the *Mimosa pudica* L. plant to curl and droop.

The time dimension examines the concept of growth and adaptation during fabrication as well as material response post-manufacturing. CNSilk presents the concept of on-demand material generation where material synthesis is modulated in response to the environment. Passive Smart Glass considers the design potentials of incorporating smart materials that respond to specific conditions in the environment.

3.3.2 On-demand Material Generation: CNSilk

Drawing inspiration from Nature's tensile systems, CNSilk (Fig 8) seeks to develop a material synthesis and fabrication approach for tensile structures where material synthesis is an integral part of the fabrication process and tensile members are dynamically generated to adapt to current environmental factors. CNSilk delves into the concept of on-demand synthesis to create tensile elements, which are dynamically adapted to the environments in which they exist.

3.3.2.1 Overview & Motivation

CNSilk explores the various possibilities and potential for weaving on a robotic platform with a focus on the creation of unique geometries and material properties introduced through variations in robotic tool-paths. Perhaps more importantly, CNSilk explores on-demand synthesis of natural fibers drawn directly from a liquid solution as required for the production of the tensile members. This process implies the integration of material generation as part of the fabrication process: beyond weaving with prefabricated fibers, this exploration seeks to weave with fibers synthesized immediately prior to deposition whose structure and properties are informed by the fabrication process itself. Synthesizing the stock material on demand affords a greater opportunity to develop a more integrated material system and fabrication approach in contrast to traditional architectural fabrication protocols that focus on cutting and reassembling discrete parts. The ability to develop and vary material properties on the fly affords greater design flexibility for the end result at multiple scales.

In the process of spinning a complete web, spiders vary not only the physical structure of the web, including its morphological features such as density, relative thickness and organization, but also its material composition. Although the protein hierarchy is generally similar across different spider silk types, the presence of various other compounds is often used to tune and enhance the silk's properties (Denny, 1976). Dragline and frame silk from which the spider suspends itself and crafts the structural spokes of the web is one of the strongest spider silks and contains higher amounts of alanine residues, which are found in the hard crystalline segments of the silk (Vollrath & Knight, 2001). Silk used for prey capture requires a lower stiffness and higher extensibility but is coated in varying drops of glue and contains higher concentrations of pyrrolidine to help retain moisture. The spider silk can be made to contain venom or pheromones or be resistant to fungi and bacteria (Vollrath, 1999). Some such as the frame silks are made to absorb energy while others transmit vibrations efficiently to act as alarm lines.

From the perspective of digital design fabrication, spider web spinning represents a form of natural additive manufacturing not unlike multi-material 3-d printing in which the end product is informed by multiple environmental factors and material optimization (Oxman, 2010). In contrast to industrial additive manufacturing methods, which generally print with compressive elements, spider webs are composed of largely tensile elements resulting in seamless structures with functionally graded material compositions.

Experiments were conducted using three general types of materials. Initial tests were done with the robotic arm using 4-ply cotton yarn wrapped on to a steel frame structure. Further experiments were conducted by weaving with nylon 6,6 synthesized and drawn from the interface of a two-phase system. Rudimentary tests were based on creating composites using cotton and Kevlar fibers drawn through resins of various mechanical properties.

3.3.2.2 Design

The robotic platform used in all automated experiments is a KUKA KR5 sixx R850 industrial 6- axis robotic arm with a reach of 0.85 m with a repeatability of 3 x 10-5 m. The arm was programmed in KUKA Robot Language (KRL) using either a KUKA KR C2 sr controller or Python scripts to convert lists of tool path points into KRL.

For all yarn weaving experiments and some nylon 6,6 experiments, 16-gauge galvanized steel wire was used to create the weaving frame. All reagents used in the nylon 6,6 synthesis were purchased from Sigma-Aldrich.

For the initial robotic weaving experiments, 4-ply cotton yarn was used as the weaving material and a galvanized steel frame with hooks spaced 0.0508 m by 0.706 m was used as a weaving frame (**Figure 23**). A holder attachment to the arm was built to contain a spool of yarn; to allow the relatively bulky holder to maneuver around the pegs, the yarn was passed through a 0.05 m long hollow tube attached to the distal tip of the holder relative to the robotic arm.

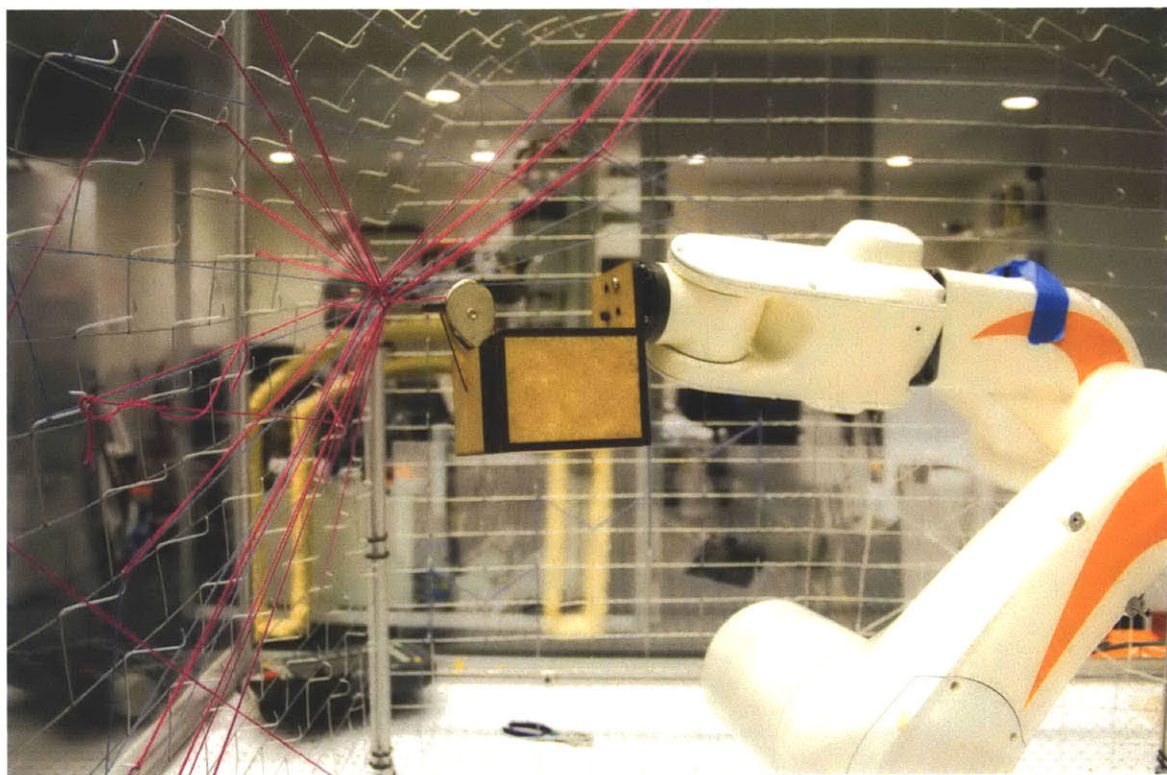


Figure 23. Image of the KUKA arm with a holder attachment containing a spool of yarn. The arm is inside a metal frame enclosure with protruding hooks serving as support for the yarn. (Tsai, Firstenberg, Laucks, Sterman, Lehnert, & Oxman, 2012)

3.3.2.3 Material Generation: Nylon 6,6

Nylon 6,6, was synthesized from adipic acid and hexamethylenediamine solutions. A 10% w/v solution of hexamethylenediamene (98%, H11696) in water with 1% w/v NaOH (reagent grade $\geq 98\%$, S5881) and a 10% w/v solution of adipoyl chloride (98%, 165212) in Hexane was used. This reaction occurs at the interface between the two solutions and, if the product (nylon) is continuously removed from the interface, the reaction is driven forward, resulting in a single strand of nylon.

Three main methods of weaving with nylon were explored. In the first method demonstrated in **Figure 24**, strands of nylon were drawn from the two-

phase nylon pre-polymer solution either by hand or by the robotic arm. Variations in strand thickness were easily controlled and achieved by modifying the speed at which the strand was drawn with faster draw times resulting in thinner strands. Thicker and stronger fibers can be created by using wider containers for the nylon synthesis and by adding certain agents such as bubble solution and glycerol to modify surface tension; Hollow cavities in the strand can be created by changing the drawn sequence and occasionally reversing the draw direction. These cavities may potentially be filled with additional materials or glue in analogy to the drop of glue found on some spider silks.

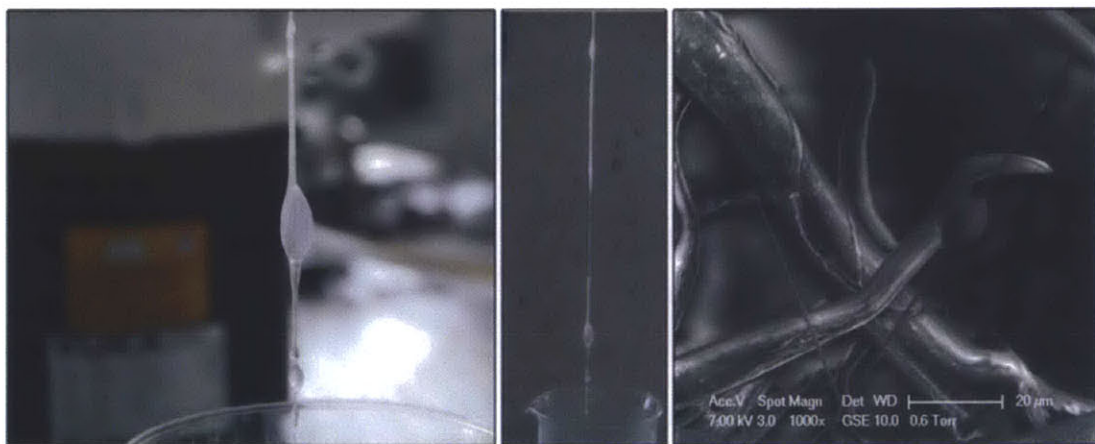


Figure 24. Nylon 6,6 being synthesized and drawn out of a 2-phase liquid system by the robotic arm (left and middle) and an electron micrograph of spider silk containing micro-droplets of glue (right). Different thicknesses and bubbles may be created by varying the draw rate and technique. (Tsai, Firstenberg, Laucks, Sterman, Lehnert, & Oxman, 2012)

In the second method seen in **Figure 25(left)**, the nylon prepolymer solution was placed on the table in front of the robotic arm and a weaving frame with pegs was attached to the arm. Nylon strands were wrapped onto the weaving frame by twisting and manipulation the robotic arm in six axis. In the third method (**Figure 25(right)**), the frame was stationary while a shallow container of the nylon prepolymer solution was manipulated such that different hooks were submerged into the solution successively, resulting in multiple strands.



Figure 25. Robotic Arm manipulating the weaving frame that the nylon is being wrapped around. The nylon prepolymer solution is resting on the table below the arm (left). Nylon threads attached to hooks on a steel frame formed by dipping the hooks into a nylon prepolymer solution. (Tsai, Firstenberg, Laucks, Sterman, Lehnert, & Oxman, 2012)

By using a method of turning and drawing, thin skin-like membranes can be created. A fixed frame constructed with MDF pegs was used and a shallow container of nylon prepolymer solution was dipped and rotated onto pair of adjacent peg, successively (**Figure 26** (left)). Formulating the nylon prepolymer solution with 50% by volume of bubble solution resulted in a stronger and larger nylon skins when drawn using multiple or cylindrical hooks (**Figure 26**(right)). Various amounts of water-based coloring agents and bubble solution may be further added to the aqueous solution to alter the optical and mechanical properties of the resulting nylon skin.



Figure 26. *Images of nylon 6,6 membranes created by turning and dipping a shallow container of nylon prepolymer onto adjacent pegs (left) and by formulating the nylon prepolymer solution using 50% bubble solution (right). In collaboration with Yoav Sterman. (Tsai, Firstenberg, Laucks, Sterman, Lehnert, & Oxman, 2012)*

Textile composites made from resins with different degrees of tensile and flexural moduli and strength were fabricated by hand in anticipation of identifying suitable fiber-resin combination to be used in the robotic weaving of functionally graded textile composites.

3.3.2.4 Discussion & Realization

In exploring the robotic creation of woven structures inspired by spider silk, the importance of material properties in the context of environment becomes increasingly clear. Spiders produce silk very sparingly, yet the use of each silk type and the design of the web overall is optimized for performance and mechanical strength.

Future work will involve the continued characterization and exploration of suitable fiber- resin systems for CNSilk as well as the incorporation of additional material factors and sensors into the system. Aside from catching prey, spiders weave silk for a large number of functions including gas exchange and filtering between the inside of a silk structure and the external environment.

In considering the robotic construction of woven structures on the architectural scale, it may be necessary to shift fabrication approaches on a more fundamental level. Spiders produce relatively giant aerial webs by allowing the environment (placement of existing support structures and direction and strength of wind) to dictate the final structure. The environment not only influences the fabrication, but also the response and adaptability of the structure throughout its lifetime. Is it possible to design a parallel artificial system that simply provides the raw construction material and relies largely on environmental factors to determine the product?

At its core, CNSilk explores the concept of material synthesis as an integral part of the fabrication process, where tensile members are dynamically generated to adapt to current environmental factors. The intent of this approach is to allow the material system to function in a less intensive way than electronically driven methods, embedding the technology into the system rather than it functioning as a supplement. Embedding environmental factors into the work-flow opens the potential for adaptation of the skin as a function of its environment. Continued development of this research could potentially be adapted to integrate material and density gradients to incorporate both structural skin and apertures through either a single or multiple materials. Future applications might include building-scale envelope systems, personal shelters, wearable artifacts and orthotics, and vehicle enclosures.

3.3.3 Environmental Response: Passive Smart Glass

3D printed objects may achieve complex geometries and material distributions designed to anticipate certain loads and stresses, but they are typically unable to continuously respond to changes in the environment. Passive Smart Glass explores the potential of combining a temperature responsive hydrogel with conventionally fabricated objects to achieve a degree of environmental response. Poly(N-isopropylacrylamide) (PNIPAM) is a thermosensitive hydrogel that is optically clear below its lower critical solution temperature (32°C) and becomes

increasingly opaque and hydrophobic when heated. In aqueous solutions, this increase in hydrophobicity results in a shrinking of the gel as water molecules are expelled from within the crosslinked network. (Hirokawa & Tanaka, 1984)

Two prototypes were created using PNIPAM as shown in Figure 27 where the hydrogel was injected between either flat or patterned panes of glass to create temperature responsive assemblies. In this example, the patterned glass was fabricated by vacuum forming but this approach is also possible for 3D printed geometries. The integration of photo cross-linkable PNIPAM copolymers into multi-material stereolithography additive manufacturing technologies could enable the fabrication of truly responsive objects, e.g. orthoses which swell and change in rigidity as a function of body temperature.

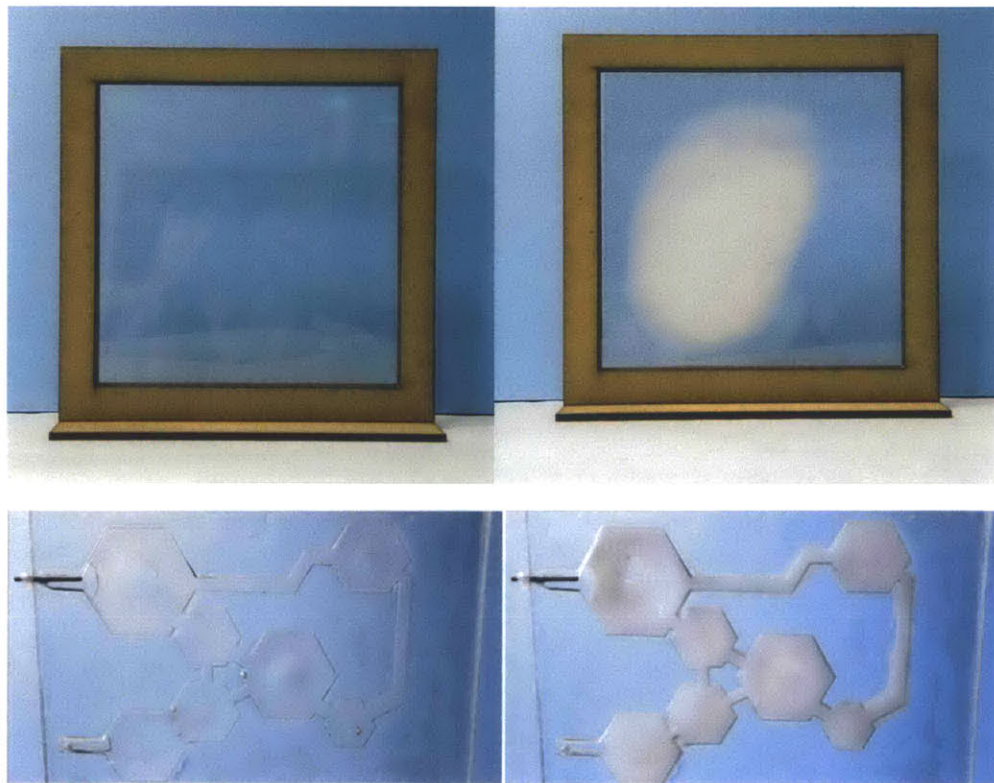


Figure 27 (top) Passive Smart Glass example created using PNIPAM sandwiched between planes of glass below (left) and above (right) critical solution temperatures. (bottom) PNIPAM injected into patterned glass. In collaboration with Dr. Michal Firstenberg. Patterned glass fabricated by Federico Mazzolini at the MIT Glass Lab.

3.4 The Information Dimension: Spatio-temporal Content Variation

3.4.1 Vision: Materials As Software

Spatiotemporal content variation within additively manufactured items may take several forms, generative or discriminative. In one approach, information is inherently embedded as part of the material; in another, the material becomes the means itself for computation and content collection. One example of the latter involves the fabrication of embedded sensors during the manufacturing process of the overall object. Using the wide range of properties of Stratasys' Digital Materials, for example, optical elements may be introduced into interactive devices to produce optical sensors, internal light guides and illumination as well as other interactive devices. In this sense, objects are prefabricated with the ability to collect and process information (Willis, Brockmeyer, Hudson, & Poupyrev, 2012).

3.4.2 Embedding Information: Material DNA

Each living organism contains many copies of a molecule that serves as the blueprint for its development and function. It is a unique identifier from which a host of information about the organism's composition, regulatory agents, and evolutionary history can be inferred. On a population-wide scale, complex evolutionary and migratory events can be identified and tracked. Technologies such as the Electronic Product Code (EPC) provide unique identifiers for objects, yet existing methods for its representation are typically confined or affixed to one part of the object.

Imagine if every single object was infused with a similar unique identifier. Given any small fragment of a car, a table, or even a vegetable, one would be able to determine where it came from, how it was made, what it was composed of, and its overall structure by analyzing its "material DNA". It leaves a microscopic trail of information everywhere it goes. An unsigned piece of furniture passed down over generations and across continents can still be traced back to its origin. A contaminated bowl of spinach need not result in a nationwide recall – every leaf of

spinach grown in the same field and processed in the same facility can be identified. Scientists in the future can accurately recreate entire objects from today using only small fragments of the original artifacts.

Rapid prototyping enables the creation of singular, unique objects as well as the fabrication of dozens of thousands of identical objects by different users across the world. The introduction of a physical, perhaps electronic information carrier, "Material DNA", within rapid prototyped objects enabling transmittal and storage of rewritable information within larger objects themselves has interesting ramifications for communicating the design or history of the artifacts. These tags could potentially be integrated into a variety of commercial manufacturing and production methods. They could be mixed into 3D printer inks and powders or perhaps injection molding materials.

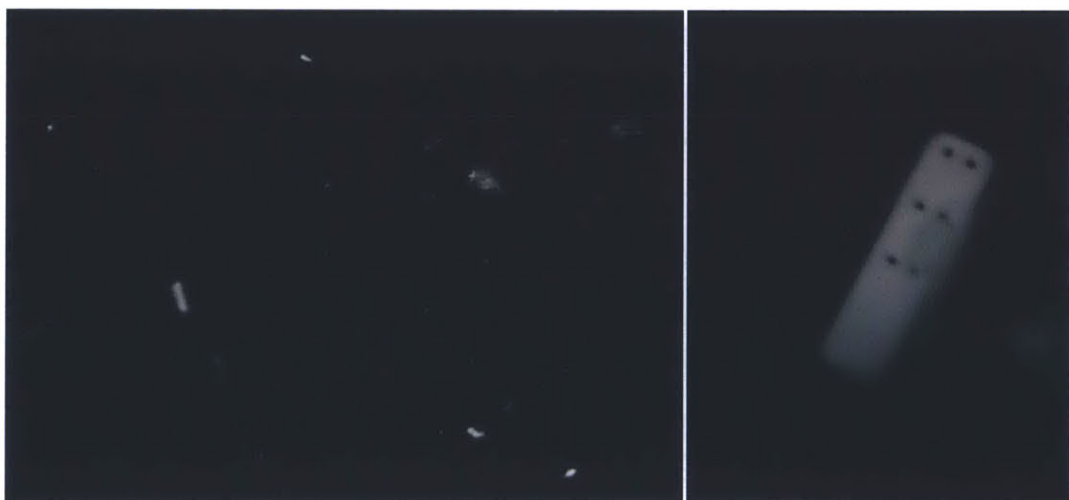


Figure 28 (left) Image of multiple fluorescent particles as seen embedded in a photopolymerized polyurethane key. (right) Close-up of particle ~200um in size.

Current preliminary research in collaboration with the Doyle Lab (MIT Chemical Engineering) has shown the ability to permanently embed microscale barcodes pervasively throughout an object during the manufacturing process using both FDM and photolithography techniques. Microscale barcodes produced using

stop flow lithography (SFL) are introduced into additive manufacturing processes either as part of a photopolymerizable resin or as part of a thermoplastic filament used fed into a Makerbot Replicator printer. Particles embedded into objects in this way may then be read using optical microscopy methods as seen in **Figure 28**.

4. Evaluation & Contributions

4.1 Theory & Methodology: Exploration of Additional Fabrication Dimensions

4.1.1 Nature: Growth, Adaptation, Evolution

In Nature, material systems are continuously evolving to meet the demands of their environment, whether through growth or through specific adaptation to external stimuli. The generation of objects occurs not through assemblies, but rather through the synthesis, secretion or subtraction of material. The relationships between the fabrication process and environmental conditions are closely integrated and in some cases – as in the construction of bird nests and aggregate systems – one and the same, creating an optimization that occurs as a result of inherent computation and analysis during generation. This work presented examples of how Nature's themes of growth, adaptation and evolution may be explored using additive manufacturing as an artificial platform in which form may be created without assembly

4.1.2 Manufacture: Defining The 4th Dimension

In its most basic sense, 3D printing refers to the deposition of a material in a layer-by-layer process. As material and process innovations allow for the creation and incorporation of additional functionality, new dimensions and approaches to design become possible. *4D Printing: Towards Biomimetic Additive Manufacturing* presents a methodology towards and system of classification of these additional design dimensions.

4.2 Technology

4.2.1 Object Representation: Bitmap Printing

The ability to physically fabricate complex material distributions using CNC platforms necessitates the ability to digitally design, store, and communicate not only geometries but also material assignment. Presented here as part of a case study for fabricating a multi-material prosthetic socket is a process for *bitmap*

printing where both part geometry and material distribution can be represented at the resolution the 3D printer. A solid, watertight socket prototype was successfully printed on a Stratasys Objet500 Connex printer using this method.

4.2.2 Platforms: CNSilk and Variable Elasticity Printer

Two fabrication platforms were developed as case studies of printing in the material and time dimensions. The first, the *Variable Elasticity Printer*, employs an active mixing and deposition approach to creating truly continuous 2-part material gradients in layered manufacturing. Gradients using elastomers, hydrogels and adhesives were made using this platform. The second, *CNSilk*, examined two themes in additive manufacturing beginning by exploring the implications of freeform printing with tensile elements and then the concept of on-demand material generation where the solid material to be deposited is synthesized in varying widths, compositions and lengths from a two-phase solution depending on the deposition conditions.

4.2.3 Systems: Material DNA

Additive manufacturing as a rapid prototyping technology enables on-demand fabrication and duplication for the layperson and provides an incredibly high degree of object customizability. As a manufacturing process where the object is built up voxel-by-voxel and layer-by-layer rather than cast, injected or subtractively manufactured from a block, it suggests the possibility of creating content or information inherent to the material itself. Material DNA is proposed as a potential system for spatio-temporal content variation and preliminary experiments were conducted to test the ability to embed and then detect microscale barcodes in materials through conventional additive manufacturing methods.

4.3 Implications in Design and Fabrication

Although there has been work in the literature to signify a potential shift, objects designed for fabrication are still typically geometrically defined as assemblies of components with different material compositions, confined to a static

form post fabrication. Case studies like the *VTS* in combination with tenants of 4D printing suggest the promise of analysis-synthesis-analysis workflows in manufacturing where environmental conditions and performance parameters are measured, and form, composition and fabrication are generated as a logical progression.

5. Conclusions

All material systems in Nature form and adapt to some extent as a result of the environment that they must operate in. In aggregate systems such as bird nests or the shells of *Difflugia*, organisms adapt their processes according to both the materials and factors present in their environment. In web and membrane systems, the composition material itself, e.g. the silk thread, is varied in addition to the geometry in accordance with both instantaneous and future factors. Living material systems continuously adapt and evolve through time as can be seen in bones and plants where changes in loading patterns may lead to additional bone or cell wall formation.

The case studies presented in Chapter 3 of this thesis in combination with the examples of 4D printing in current manufacturing discussed in Section 1.4 comprise only the beginnings of a cursory exploration into the potential of additional design dimensions in additive manufacturing. In the material dimension, the ability to design, control and modulate material property and behavior across spatial scales, may promote higher efficiencies and more effective additive manufacturing platforms while resulting in artifacts designed to interact with natural systems in a way that complements and enhances their material properties. Artifacts that may respond to forces or adapt throughout the time dimension in a predesigned fashion and the ability to incorporate spatiotemporal content variation may be the first steps towards fabricating with, by and as Nature. Altogether, 4D printing seeks to become a platform for bio-inspired additive manufacturing design that reaches beyond mere mimicry to create objects that truly interface with natural systems and contribute a new level of function.

References

- Adams, J., Duoss, E., Malkowski, T., Motala, M., Ahn, B., Nuzzo, R., et al. (2011). Conformal Printing of Electrically Small Antennas on Three-Dimensional Surfaces. *Advanced Materials*, 23 (11), 1335-1340.
- Agache, P., Monneur, C., Leveque, J., & De Rigal, J. (1980). Mechanical Properties and Young's Modulus of Human Skin in Vivo. *Archives of Dermatological Research*, 269 (3), 221-232.
- Ahn, S.-H., Montero, M., Odell, D., Roundy, S., & Wright, P. (2002). Anisotropic Material Properties of Fused Deposition Modeling ABS. *Rapid Prototyping Journal*, 8 (4), 248-257.
- Arruda, E., & Boyce, M. (1993). A Three-Dimensional Constitutive Model for The Large Stretch Behavior of Rubber Elastic Materials. *J. Mech. Phys. Solids*, 41, 389-412.
- Becker, N., Oroudjev, E., Mutz, S., Cleveland, J., Hansma, P., Hayashi, C., et al. (2003). Molecular Nanosprings in Spider Capture-Silk Threads. *Nature Materials*, 2, 278-283.
- BIschoff, J., Arruda, E., & Grosh, K. (2000). Finite Element Modeling of Human Skin Using an Isotropic, Nonlinear Elastic Constitutive Model. *Journal of Biomechanics*, 33, 645-652.
- Buswell, R., Soar, R., Gibb, A., & Thorpe, A. (2007). Freeform Construction: Mega-scale Rapid Manufacturing. *Automation in Construction*, 16 (2), 224-231.

Carter, D., Fyhrie, D., & Whalen, R. (1987). Trabecular Bone Density and Loading History: Regulation of Connective Tissue Biology by Mechanical Energy. *Journal of Biomechanics*, 20 (8), 278-283.

Chen, Y. (2008). *Nonlinear Stochastic System Identification Techniques for Biological Tissues*. MS Thesis, Massachusetts Institute of Technology.

Convery, P., & Buis, A. (1998). Conventional Patellar-Tendon-Bearing (PTB) Socket/Stump Interface Dynamic Pressure Distributions Recorded During the Prosthetic Stance Phase of Gait of a Transtibial Amputee. *Prosthetics and Orthotics International*, 22, 193-198.

Cooke, W., Tomlinson, R., Burguete, R., Johns, D., & Vanard, G. (2011). Anisotropy, Homogeneity and Ageing in an SLS Polymer. *Rapid Prototyping Journal*, 17 (4), 269-279.

Denny, M. (1976). The Physical Properties of Spider's Silk and Their Role in the Design of Orb-Webs. *Experimental Biology*, 65, 483-506.

Doblare, M., & Garcia-Aznar, J. (2008). Modelling Living Tissues: Mechanical and Mechanobiological Aspects. *Progress in Industrial Mathematics at ECMI*, 3-8.

Elsner, P., Berardesca, K., & Wilhelm, K. M. (2002). *Bioengineering of the Skin: Skin Biomechanics*. CRC Press.

Fromm, J., & Eschrich, W. (1988). Transport Processes in Stimulated and Non-stimulated Leaves of Mimosa pudica. *Trees*, 2 (1), 7-17.

Gibson, L. (1985). The Mechanical Behaviours of Cancellous Bone. *Journal of Biomechanics*, 18 (5), 317-328.

Gosline, J., Demont, M., & Denny, M. (1986). The Structure and Properties of Spider Silk. *Endeavour*, 10 (1), 37-43.

Hansell, M. (2000). *Bird Nests and Construction Behavior*. Cambridge University Press.

Hayes, W., Keer, L., Hermann, G., & Mockros, L. (1972). A Mathematical Analysis for Indentation Tests of Articular Cartilage. *Journal of Biomechanics*, 5, 541-551.

Herbert, N., Simpson, D., Spence, W., & Ion, W. (2005). A Preliminary Investigation Into the Development of 3D Printing of Prosthetic Sockets . *Journal of Rehabilitation Research and Development*, 42 (2), 141-146.

Hirokawa, Y., & Tanaka, T. (1984). Volume Phase Transition in a Nonionic Gel. *The Journal of Chemical Physics*, 81 (12), 6379-6380.

Hu, T., & Desai, J. (2004). Characterization of soft-tissue material properties: Large deformation analysis. In *Medical Simulation: Lecture Notes in Computer Science* (Vol. 3078, pp. 28-37). Springer.

Hu, T., & Desai, J. (2004). Soft-Tissue Material Properties Under Large Deformation: Strain Rate Effect. *Proceedings of IEEE Engineering Medical Biol. Soc.*, 4, pp. 2758-2761.

Huiskes, R., Ruimerman, R., van Lenthe, G., & Janssen, J. (2000). Effects of Mechanical Forces on Maintenance and Adaptation of Form in Trabecular Bone. *Nature*, 405 (6787), 704-706.

Johannesson, A., Larsson, G., & Oberg, T. (2004). From Major Amputation to Prosthetic Outcome: a Prospective Study of 190 Patients in a Defined Population. *Prosthetics and Orthotics International*, 28, 9-21.

Klasson, B. (1995). Carbon Fibre and Fibre Lamination in Prosthetics and Orthotics: Some Basic Theory and Practical advice for the Practitioner. *Prosthetics and Orthotics International*, 19, 74-91.

Korochkina, T., Claypole, T., & Gethin, D. (2005). Choosing Constitutive Models for Elastomers used in Printing Processes. In *Constitutive Models for Rubber IV* (pp. 431-435). UK: Balkema Publishers.

Laferrier, J., & Gailey, R. (2010). Advances in Lower-Limb Prosthetic Technology . *Physical Medicine and Rehabilitation Clinics of North America , 21* (1), 87-110.

Levy, G., Schindel, R., & Kruth, J. (2003). Rapid Manufacturing and Rapid Tooling with Layer Manufacturing (LM) Technologies, State of the Art and Future Perspectives. *CIRP Annals - Manufacturing Technology , 52* (2), 589-609.

Mak, A., Liu, G., & Lee, S. (1994). Biomechanical Assessment of Below- Knee Residual Limb Tissue . *Journal of Rehabilitation Research and Development , 31* (3), 188-198.

Malm, M., Samman, M., & Serup, J. (1995). In Vivo Skin Elasticity of 22 Anatomical Sites. *Skin Research and Technology , 1* (2), 61-67.

Marlow, R. (2003). A General First-Invariant Hyperelastic Constitutive Model. . In J. Busfield (Ed.), *Constitutive Models for Rubber* (pp. 157-160). UK: AA Balkema Publishers.

Melchels, F., Feijen, J., & Grijpma, D. (2010). A Review on Stereolithography and Its Applications in Biomedical Engineering. *Biomaterials , 31* (24), 6121-6130.

Miyamoto, Y., Kaysser, W., Rabin, B., Kawasaki, A., & Ford, R. (1999). *Functionally Graded Materials: Design, Processing and Applications*. Springer.

Mooney, M. (1940). A Theory of Large Elastic Deformation. *Journal of Applied Physics , 11* (9).

Ogden, R. (1984). *Non-Linear Elastic Deformations*. Chichester, UK: Ellis Horwood.

Ogden, R., Saccomandi, G., & Sgura, I. (2004). Fitting Hyperelastic Model to Experimental Data. *Computational Mechanics , 34*, 484-502.

Oxman, N. (2010). *Material-based Design Computation*. PhD Thesis, Massachusetts Institute of Technology.

Oxman, N. (2010). Structuring Materiality: Design Fabrication of Heterogeneous Materials. *Architectural Design*, 80 (4), 78-85.

Oxman, N. (2011). Variable Property Rapid Prototyping. *Journal of Virtual and Physical Prototyping (VPP)*, 6 (1), 3-31.

Oxman, N., & Hart, A. (2008). *Microstructure Research for Building Skins*. Holcim Awards for Sustainable Construction.

Oxman, N., Keating, S., & Tsai, E. (2011). Functionally Graded Rapid Prototyping. *Proceedings of VRAP: Advanced Research in Virtual and Rapid Prototyping in: "Innovative Developments in Virtual and Physical Prototyping"*.

Oxman, N., Tsai, E., & Firstenberg, M. (2012). Digital Anisotropy. *Journal of Virtual and Physical Prototyping*.

Patil, L., Dutta, D., Bhatt, A., Jurrens, K., Lyons, K., & Pratt, M. (2002). A Proposed Standards-Based Approach for Representing Heterogeneous Objects for Layered Manufacturing. *Rapid Prototyping Journal*, 8 (3), 134-146.

Pellacani, G., & Seidenari, S. (1999). Variations in Facial Skin Thickness and Echogenicity with Site and Age. *Acta Derm Venereol*, 79, 366-369.

Phillip, J., & Johnson, K. (1981). Tactile Spatial Resolution. III. A Continuum Mechanics Model of Skin Predicting Mechanoreceptor Responses to Bars, Edges, and Gratings. *Journal of Neurophysiology*, 46 (6), 1204-1225.

Pierard, G., & Lapierre, C. (1977). Physiopathological Variations in the Mechanical Properties of Skin. *Archives of Dermatological Research*, 260 (3), 231-239.

Rossiter, J., Walters, P., & Stoimenov, B. (2009). Printing 3D Dielectric Elastomer Actuators for Soft Robotics. *11th SPIE Electroactive Polymer Actuators and Devices Conference*.

Sanders, J. D. (1993). Normal and Shear Stresses on a Residual Limb in a Prosthetic Socket During Ambulation: Comparison of Finite Element Results with Experimental Measurements. *Journal of Rehabilitation Research*, 30 (2), 191-204.

Sanders, J., Harrison, D., Allyn, K., & Myers, T. (2009). Clinical Utility of In-Socket Residual Limb Volume Change Measurements: Case Study Result. *Prosthetics and Orthotics International*, 33 (4), 178-190.

Sengeh, D. (2012). *Advanced Prototyping of Variable Impedance Prosthetic Sockets for Trans-tibial Amputees: Polyjet Matrix 3D Printing of Comfortable Prosthetic Sockets Using Digital Anatomical Data*. MS Thesis, Massachusetts Institute of Technology.

Sewell, P., Noroozi, S., Vinney, J., & Andrews, S. (2000). Developments in the Trans-Tibial Prosthetic Socket Fitting Process: A Review of Past and Present Research. *Prosthetics and Orthotics International*, 24 (2), 97-107.

Sheng, W., Xi, N., Chen, H., Chen, Y., & Song, M. (2003). Surface Partitioning in Automated CAD-Guided Tool Planning for Additive Manufacturing. *IEEE/RSJ International Conference on Intelligent Robots and Systems*, 2, pp. 2072-2077.

Silver-Thorn, M., Steege, J., & Childress, D. (1996). A Review of Prosthetic Interface Stress Investigations. *Journal of Rehabilitation Research and Development*, 33 (3), 253-266.

Staker, M., Ryan, K., & LaBat, K. (2009). Medicine and Design Investigate Residual Limb Volume Fluctuation: 3 Case Studies. *Australasian Medical Journal*, 12 (1), 156-161.

Thomas, B. (1983). The Plain-Fronted Thornbird: Nest Construction, Material Choice and Nest Defense Behavior. *The Wilson Bulletin*, 95 (1), 106-117.

Tibbits, S. (2013). 4D Printing: Multi-Material Shape Change. (B. Sheil, Ed.) *High-Definition: Negotiating Zero Tolerance, Architectural Design Journal*.

Toohey, K., Sottos, N., Lewis, J., Moore, J., & White, S. (2007). Self-healing Materials With Microvascular Networks. *Nature Materials*, 6, 581-585.

Treloar, L. (1948). Stresses and Birefringence in Rubber subjected to General Homogenous Strain. *Proceedings of the Physical Society*, 60 (2).

Tsai, E., & Oxman, N. (2013). 4D Printing: Towards Biomimetic Additive Manufacturing. *Proceedings of the Additive Manufacturing and 3D Printing International Conference*.

Tsai, E., Firstenberg, M., Laucks, J., Sterman, Y., Lehnert, B., & Oxman, N. (2012). CNSILK: Spider-Silk Inspired Robotic Fabrication. *Proceedings of Rob-Arch 2012: Robotic Fabrication in Architecture, Art and Design*.

Vollrath, F. (1999). Biology of Spider Silk. *International Journal of Biological Macromolecules*, 24, 81-88.

Vollrath, F., & Knight, D. (2001). Liquid Crystalline Spinning of Spider Silk. *Nature*, 410, 541-548.

Walters, P., & McGoran, D. (2011). Digital Fabrication of Smart Structures and Mechanism: Creative Applications in Art and Design. *The Society for Imaging Science and Technology*, 185-188.

Walters, P., & Rossiter, J. (2008). Three-Dimensional Fabrication of Smart Actuators: Design Applications. *NIP24: International Conference on Digital Printing Technologies and Digital Fabrication*.

Weiss, J., Gardiner, J., & Quapp, K. (1995). Material Models for the Study of Soft Tissue Mechanics . *Proceedings of the International Conference on Pelvin and Lower Extremity Injuries*, (pp. 249-261).

Weiss, L., Merz, R., Prinz, F., Neplotnik, G., Oadmanabhan, P., Schultz, L., et al. (1997). Shape Deposition Manufacturing of Heterogeneous Structures. *Journal of Manufacturing Systems*, 16 (4), 239-248.

Willis, K., Brockmeyer, E., Hudson, S., & Poupyrev, I. (2012). Printed Optics: 3D Printing of Embedded Optical Elements for Interactive Devices. *Proceedings of the 25th Annual ACM Symposium on User Interface Software and Technology*, (pp. 589-598).

Xu, H., Teoh, S., & Sun, Y. (2002). *Computational Models for Mechanical Deformation of Soft Tissues of the Central Nervous System*. Technical Reports, Purdue University Computer Science.